Computational investigation of atomic structure and spectral features of Ti I and Ti II using SUPERSTRUCTURE code

A dissertation submitted in partial fulfillment of the requirement for a Master of Science in the Department of Physics, University of Dhaka

Submitted by

MD. MEHEDI FAYSAL

Examination Roll: 107827

Registration No: 2016-813-414 (2016-17)

M.S. Session: 2020-2021

Department of Physics, University of Dhaka

September, 2023

Date: 13.09.2023

In forwarding the thesis entitled **"Computational investigation of atomic structure and spectral features of Ti I and Ti II using SUPERSTRUCTURE code."** in partial fulfillment for the degree of Master of Science in Physics at the University of Dhaka, I, hereby certify that, **"Md. Mehedi Faysal"** with the **examination Roll No: 107827** and **Reg. No: 2016-813-414 (2016-2017)** has completed the research work as a full time student and the thesis contains results of his investigation conducted during the period he worked as an **M. S. (Thesis), Session-2020-2021** student under my supervision.

Thesis Advisor
Professor Sultana N. Nahar
Department of Astronomy, McPherson Lab,
The Ohio State University
United State of America

Acknowledgements

I extend my heartfelt gratitude to several individuals and organizations who have played pivotal roles in shaping the trajectory of my academic journey.

First and foremost, I would like to express my sincere appreciation to the **Ohio Super Computer** for generously providing me with free access to their server resources. This access was instrumental in facilitating the computational aspects of my research, enabling me to carry out complex simulations and data analysis.

I am deeply indebted to the **Ohio State University** for their unwavering support, which included arranging unlimited Zoom sessions. This invaluable resource allowed me to stay connected with my advisor, fostering collaborative discussions and knowledge exchange.

I extend my profound thanks to my esteemed advisor, **Professor Sultana N. Nahar**, whose mentorship has been a guiding light throughout my thesis journey. Her expertise in the field of Atomic Astrophysics has not only enriched my knowledge but also served as the bedrock upon which my research was built. Her unwavering dedication and insightful teachings have been invaluable to me.

I would also like to acknowledge the contributions of my supervisor, **Professor Dr. Ishtiaque Syed**, who provided me with the opportunity to connect with Professor Nahar. His support and mentorship have been instrumental in facilitating a fruitful academic journey.

Finally, my heartfelt gratitude goes out to my parents, whose unwavering support and encouragement have been a constant source of strength throughout my academic endeavors. Their belief in my potential and their presence during both highs and lows have been my greatest motivation.

To each of these individuals and institutions, I offer my sincerest thanks for their contributions to my academic and personal growth.

Abstract

For my M.Sc. thesis research, I have utilized advanced computational techniques to calculate energy levels, transition probabilities, and oscillator strengths and lifetimes for Titanium (Ti) ions, Ti I and Ti II. I employed SUPERSTRUCTURE, an atomic structure code which implements Thomas-Fermi-Dirac-Amaldi potential for the electron-electron interaction and takes into account relativistic effects in Breit-Pauli approximation. I studied various types of transitions, allowed electric dipole (E1), and forbidden electric quadrupole (E2), electric octupole (E3), magnetic dipole (M1), and magnetic quadrupole (M2). I compared the energies and oscillator strengths with those available at the compiled tables of National Institute of Standards and Technology (NIST) for accuracy determination. We also computed the lifetimes of levels obtained using a different code called LIFETIME. I have presented lifetimes for 5 fine structure levels of Ti I and 16 fine structure levels of Ti II. We studied the spectral features of both Ti I and Ti II to determine the dominating ranges of wavelengths for strong spectral lines for possible detection in astrophysical spectra and applications. For Ti I, we investigated ten different electron configurations ($3d^2 4s^2$, $3d^3 4s$, $3d^2 4s4p$, $3d^3 4p$, $3d^3 4d$, $3d^3 4f$, $3d^3 5s$, $3d^4$, $3d4s^2 4p$, $3d^2 4s4d$). These configurations resulted in 839 fine structure energy levels, enabling us to calculate a total of 372,775 transitions of all allowed and forbidden types. For Ti II, we worked with a set of ten electron configurations ($3p^6 3d^2 4s$, $3p^6 3d^3$, $3p^6 3d4s^2$, $3p^6 3d^2 4p$, $3p^6 3d^2 4d$, $3p^6 3d^2 4f$, $3p^6 3d4s4p$, $3p^6 3d4s5p$, $3p^5 3d^4$, $3p^4 3d^5$). These configurations yielded 969 fine structure energy levels and a total of 474,320 allowed and forbidden transitions. I have presented tables of comparative studies of our results with the NIST data and discussed the comparisons. Our results show fair to good agreement. Large discrepancies, particularly with high lying energy levels, are also noted. We conducted the spectral analysis of Ti I and Ti II by plotting oscillator strength against wavelength. The figures are presented showing the strength of lines of these two ions at wavelengths that can be used for detection, analysis and modeling of astrophysical and laboratory plasma. Our research provides valuable insights into the atomic properties and spectral behavior of Ti I and Ti II, contributing to a deeper understanding of these elements.

Table of Contents

List of figures

Chapter 1

Introduction

In the ever-evolving landscape of atomic and molecular physics, the exploration of the fundamental properties of matter continues to stand as a testament to human curiosity and scientific progress. Within this dynamic domain, the study of atoms and ions remains a cornerstone, offering insights into the complex dance of electrons and the quantum mechanical phenomena that underpin our physical reality. Among the elements that have consistently beckoned scientists and researchers due to their intriguing electronic configurations and versatile applications, titanium (Ti) emerges as an enticing subject of study. In this thesis, we embark on a compelling expedition into the realm of titanium chemistry, focusing our gaze on Ti(I) (neutral titanium) and Ti(II) (Ti^+) ions. Our overarching aim: to unveil the enigmatic properties of these ions, with a particular emphasis on their oscillator strength, energy levels, and transition probabilities, utilizing the powerful atomic structure code, SUPERSTRUCTURE.

1. 1 Astrophysical Significance of studying Titanium

- **Stellar Composition Analysis:** Stars are essentially gigantic nuclear reactors where various nuclear reactions occur. The elements present in a star, including Ti ions, emit specific spectral lines when they undergo transitions between energy states. By accurately determining the atomic data of Ti ions, such as transition probabilities and oscillator strengths, astronomers can precisely identify and quantify the amount of titanium and other elements in stars. This, in turn, helps in characterizing the chemical composition of stars, a critical factor in understanding their evolution and life cycles.
- **Stellar Temperature Determination:** The temperature of a star influences the distribution of electrons in its atomic and ionic states. Accurate atomic data for Ti ions allows astronomers to analyze the intensity and shape of spectral lines produced by Ti ions in a star's spectrum. By comparing these lines to theoretical models that incorporate your research data, astronomers can better estimate the temperature of stars. This is invaluable

for classifying stars, understanding their evolutionary stages, and determining their luminosities.

- **Stellar Evolution Models:** Stellar evolution models rely on accurate atomic data to simulate the life cycles of stars. Our research can enhance the precision of these models by providing improved atomic data for Ti ions. This, in turn, allows for more accurate predictions of how stars evolve, including their lifetimes, size changes, and eventual fates (e.g., becoming supernovae or evolving into white dwarfs).
- **Astrophysical Spectroscopy**: Observational astronomers use spectroscopy to collect data on distant celestial objects. Your research can benefit these astronomers by providing them with a more comprehensive and precise database of Ti ions' atomic properties. This improved data can lead to more accurate interpretations of observed spectra, allowing astronomers to infer crucial information about the stars, galaxies, and other cosmic objects they study.
- **Cosmic Abundance Studies:** Understanding the abundance of elements like titanium in different regions of the universe is vital for cosmological studies. By contributing to the accuracy of atomic data for Ti ions, Our research indirectly aids in determining the cosmic abundance of titanium. This information can shed light on the history of element formation in the universe.
- **Planetary Nebulae:** Ti ions are also found in the spectra of planetary nebulae, which are remnants of stars that have exhausted their nuclear fuel. Accurate atomic data is essential for analyzing the spectra of these nebulae. Our research can facilitate a better understanding of the chemical composition and physical conditions within planetary nebulae, providing insights into the late stages of stellar evolution.

1. 2 Titanium in Red giants

Red giants, massive stars in the later stages of their evolution, exhibit a fascinating array of elemental compositions, and one of the notable elements found in these celestial giants is titanium (Ti). In red giants, like those studied in the cosmos, titanium is produced through various nucleosynthesis processes. During the helium-burning phase of a red giant's life cycle, helium fuses into heavier elements, including titanium, through a series of nuclear reactions. This titanium

enrichment has significant implications for the chemical makeup of the universe, as it contributes to the formation of elements that eventually find their way into planetary systems and, potentially, the building blocks of life. Moreover, the presence of titanium in red giants is of interest to astronomers and astrophysicists studying the evolution of stars and the synthesis of elements within these stellar giants, shedding light on the intricate processes that shape the cosmos.

Here are a few notable red giants where the presence of Titanium ions has been observed:

- **Arcturus (Alpha Boötis):** Arcturus is one of the brightest stars in the night sky and is classified as a K-type giant. It exhibits Ti lines in its spectrum, making it a prominent example of a red giant containing titanium [1].
- **Aldebaran (Alpha Tauri):** Aldebaran is the brightest star in the constellation Taurus and is also a K-type giant. Titanium lines are detectable in its spectrum [2].
- **Betelgeuse (Alpha Orionis):** Betelgeuse is a red supergiant rather than a red giant, but it is a noteworthy example of a massive evolved star. Titanium, among other elements, is present in its spectrum. Betelgeuse is famous for its variability and its prominent place in the constellation Orion [3].
- **Mira (Omicron Ceti):** Mira is a well-known variable star that undergoes pulsations, causing its brightness to change over time. It is a red giant with Ti lines present in its spectrum. Mira is significant for its contribution to our understanding of stellar variability[4].

  .

1. 3 Titanium (Ti) in exoplanets

Titanium (Ti) is an element that can be found in the compositions of exoplanets, but its presence and abundance can vary depending on several factors. Here's a brief overview of the role of titanium in exoplanets:

- **Rocky Exoplanets**: Titanium is a common element in rocky materials on Earth and in our solar system. Exoplanets that are rocky in nature, similar to Earth or Mars, can contain titanium as a component of their crusts and mantles. The abundance of titanium in these exoplanets depends on their formation and subsequent geological processes.

- **Chemical Composition**: The abundance of titanium in an exoplanet's crust and mantle depends on the chemical composition of the protoplanetary disk from which it formed. Different regions of a protoplanetary disk can have varying levels of titanium, which can influence the composition of the resulting exoplanets.
- **Stellar Metallicity**: The metallicity of the host star can also play a role in the composition of exoplanets, including the presence of titanium. Metallicity refers to the abundance of elements heavier than hydrogen and helium in a star. Stars with higher metallicity are more likely to have exoplanets with rocky compositions containing elements like titanium.
- **Exoplanet Formation:** The process of exoplanet formation can influence the distribution of elements like titanium within a planetary system. Rocky exoplanets can accrete material from the protoplanetary disk, and the availability of titanium-containing dust and solids during this process can affect the exoplanet's composition.
- **Observation and Characterization:** Detecting the presence of titanium in exoplanets often relies on indirect methods such as spectroscopy. Astronomers analyze the light from a host star as it passes through an exoplanet's atmosphere or is reflected off its surface. Specific spectral features related to titanium or other elements can be used to infer their presence.
- **Exoplanetary Atmospheres:** Titanium can also be present in the atmospheres of certain exoplanets. For instance, in hot Jupiter-type exoplanets (gas giants with high temperatures), titanium oxide (TiO) has been detected in their atmospheres. TiO can influence the temperature structure and spectral properties of these atmospheres.
- **Exoplanetary Research:** Researchers studying exoplanets aim to determine their compositions and properties. Understanding the presence and abundance of elements like titanium in exoplanets provides insights into their formation and evolution. It can also help us categorize exoplanets into different classes based on their composition and atmospheric characteristics. Atmospheres of certain exoplanets through spectroscopic observations.

There exist a number of documented cases in the field of exoplanetary research wherein the element titanium (Ti) has been successfully detected

- **WASP-19b:** Another hot Jupiter exoplanet, WASP-19b, has been found to have TiO in its atmosphere. It's a transiting exoplanet located about 815 light-years away from Earth [5].
- **KELT-9b:** KELT-9b is an extremely hot gas giant exoplanet orbiting a very hot and massive host star. TiO has been detected in its atmosphere, and this exoplanet is known for its scorching temperatures [6].

1. 4 Titanium in Large Magellanic cloud (LMC)

The Large Magellanic Cloud (LMC) is a satellite galaxy of our Milky Way and is located in the southern hemisphere. It is a prominent target for astronomers studying distant galaxies and stellar populations. Titanium (Ti) is one of many elements found in the stars of the LMC[7]. Here's some information about the presence of Ti in the LMC:

- **Stellar Composition:** The LMC contains a diverse population of stars, ranging from massive young stars to older, evolved ones. These stars have varying chemical compositions, including the presence of elements like titanium. The abundance of Ti in LMC stars can vary from star to star.
- **Chemical Abundance Studies:** Astronomers have conducted spectroscopic studies of stars in the LMC to determine their chemical compositions, including the abundance of elements like titanium. These studies aim to understand the metallicity of the LMC's stellar population, which provides insights into its formation history and evolution.
- **Stellar Evolution:** The LMC serves as an important laboratory for studying stellar evolution. By analyzing the chemical compositions of LMC stars, astronomers can gain insights into the nucleosynthesis processes that have occurred in this galaxy, including the production of elements like titanium through various stages of stellar evolution.

- **Galactic Structure:** The chemical composition of stars in the LMC is essential for understanding the galaxy's overall structure and history. Studying the distribution of elements like titanium helps astronomers map the LMC's stellar populations and investigate its interaction with the Milky Way.

Figure 1.1: Large Magellanic Cloud

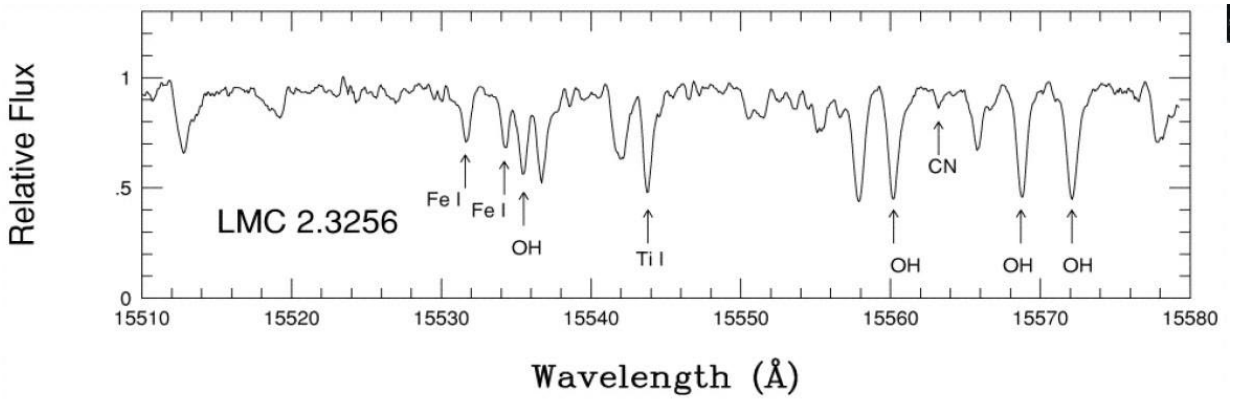

Figure 1.2: Ti I in LMC spectra. Ti line at 15544 Å

- **Supernovae and Stellar Explosions:** Titanium is produced and ejected into space during the explosive deaths of massive stars in supernova events. By studying the presence of titanium in the LMC's interstellar medium, astronomers can learn about the history of supernova explosions in this galaxy.
- **Astronomical Observations:** Observations of the LMC, including spectroscopic data, have revealed the presence of titanium lines in the spectra of its stars. These lines are used to determine the chemical composition of LMC stars and provide insights into their physical properties.

Overall, titanium is one of the many elements that astronomers study in the Large Magellanic Cloud to better understand the galaxy's stellar populations, chemical history, and role in the broader context of galaxy formation and evolution. The LMC continues to be a valuable target for observational and theoretical studies in the field of astrophysics.

1. 5 Empowering Research with SUPERSTRUCTURE (An atomic structure code)

The relentless pursuit of knowledge has led to the development of advanced computational tools that allow us to probe deeper into the atomic and molecular worlds. SUPERSTRUCTURE, a specialized atomic structure code, stands as a formidable instrument in this endeavor. It empowers us to explore the intricate electronic structures of atoms and ions with unprecedented precision and comprehensiveness. Our journey to unravel the quantum mechanical secrets of Ti(I) and Ti(II) ions takes flight on the wings of this exceptional computational tool.

1. 6 Tripartite Research Goals

This thesis is meticulously structured around three interrelated objectives:

I. **Determining Energy Levels:** Our primary goal within this study is to accurately determine the energy levels associated with Ti(I) (neutral titanium) and Ti(II) (singly ionized titanium) ions. This objective entails precise calculations facilitated by the powerful SUPERSTRUCTURE code. With this specialized computational tool, our aim is to quantitatively ascertain the energies corresponding to various electronic states and

illuminate the electronic configurations of these ions. This foundational pursuit serves as the bedrock of our research, providing us with a comprehensive understanding of the energy characteristics intrinsic to Ti(I) and Ti(II) ions. It is through this meticulous process that we gain valuable insights into the quantum mechanical behaviors of these ions, forming the essential foundation upon which our investigation is built.

II. **Navigating Transition Probabilities:** Our second mission delves into the labyrinthine world of transition probabilities for electronic transitions within Ti(I) and Ti(II) ions. Harnessing the computational prowess of the SUPERSTRUCTURE code, we aim to unveil the complexities of particle interactions, leading to a profound understanding of the relative strengths of various transitions and their consequential impact on observed spectra.

III. **Unveiling Oscillator Strengths:** At the heart of our expedition lies the meticulous determination of oscillator strengths—an elemental parameter that quantifies the probability of electronic transitions. Through the precision and finesse of the SUPERSTRUCTURE code, we intend to unveil the quantum mechanical intricacies governing these transitions, shedding light on the profound subtleties of Ti(I) and Ti(II) ions.

1. 7 Significance and Innovation

This research holds profound significance on multiple fronts. Firstly, it enriches our foundational knowledge of atomic and molecular properties, providing a more profound understanding of the electronic intricacies of Ti(I) and Ti(II) ions. Secondly, the application of the SUPERSTRUCTURE code in this study symbolizes a paradigm shift in computational methodologies, opening new horizons for scientific exploration. Moreover, the outcomes of this research carry the potential to catalyze innovation in materials science, spectroscopy, and advanced technological applications, forging a path toward new scientific discoveries and technological advancements.

1. 8 Navigating the Thesis Landscape

The landscape of this thesis unfolds as follows:

Chapter 2 provides an in-depth review of the relevant literature, highlighting previous studies on titanium ions and their spectroscopic properties.

Chapter 3 and Chapter 4 delve into the theoretical framework related to our research.

Chapter 5 discusses the computational methodologies that underpin our research, elucidating the principles and capabilities of the SUPERSTRUCTURE code.

Chapter 6 presents the results of our calculations, including the energy tables, transition probabilities, and oscillator strengths for Ti(I) and Ti(II) ions and offers a comprehensive analysis of the findings and their implications

Finally, Chapter 7 serves as the culmination of our scientific odyssey, summarizing our groundbreaking discoveries, accentuating their significance, and charting new horizons for future research.

.

Chapter 2

Literature review

2. 1 For Ti I

1930s-1940s: Early Study of Titanium's Atomic Energy Levels

In the early 1930s, the study of titanium's atomic energy levels began with the compilation by Bacher and Goudsmit in 1932[8]. At that time, only the first four spectra out of the total 22 spectra of titanium had been systematically studied, reflecting the limited state of knowledge. Progress was made by 1949 when Moore [9]compiled data for the first 13 spectra of titanium, signifying a substantial improvement in our understanding of titanium's atomic energy levels. During this era, oxygen was the heaviest atom for which some energy levels for all stages of ionization were known, emphasizing the challenges of studying heavier elements.

1970s-1980s: Infrared Spectroscopy and Titanium I Oscillator Strengths

In more recent years, the significance of infrared (IR) stellar spectroscopy has grown substantially. This growth is primarily attributed to advancements in IR detectors in both ground-based and satellite-based spectrographs. However, the analysis of costly IR astrophysical spectra has been limited primarily to the examination of molecular bands and a restricted set of atomic transitions in the near IR spectrum. This limitation arises from the absence of precise laboratory-derived atomic oscillator strengths in the IR range. This deficiency is particularly pronounced when studying cool stars and brown dwarfs, as their energy emission peaks within the IR spectrum (Lyubchik et al., 2004)[10]

The acquisition of precise oscillator strengths for specific neutral atoms is essential for determining critical stellar properties, including effective temperature, metallicity, and surface gravity (Lyubchik et al., 2004)[10].

The existing laboratory atomic database for Titanium I (Ti I) in the IR spectral range presents a notable deficiency. The longest wavelength spectral line for Ti I with a measured oscillator strength is recorded at 1.06 μm Whaling et al. in 1977 [11]. Beyond this wavelength, available oscillator strengths are derived from the semi-empirical calculations of Kurucz in 1995 [12].

However, calculating theoretical and semi-empirical oscillator strengths with the required precision for accurate abundance determinations is a formidable challenge, often accompanied by uncertainties ranging from 10 to 20 percent. This challenge becomes particularly significant when dealing with weak transitions, which may be the only viable lines for comprehensive astrophysical spectrum analysis.

1980s-1990s: Progress in Ti I Oscillator Strengths

The most comprehensive compilation of Ti I oscillator strengths to date was conducted by Martin et al. in 1988 [13]. This compilation spanned from the visible to the near-infrared (IR) and incorporated studies by Smith & Kühne in 1978, as well as Blackwell et al. in 1982a, 1982b, and 1983.[14][15]

It's important to note that the oscillator strengths initially determined by Blackwell and colleagues underwent re-examination by Grevesse et al. in 1989, which recommended an upward adjustment of these values by 0.056 dex, equivalent to a 14 percent increase [16].

Subsequently, Nitz et al. in 1998 contributed to the field by publishing experimentally measured oscillator strengths, introducing uncertainties of approximately 10 percent for certain even parity levels [17].

Additionally, various studies in the 1980s and 1990s employed time-resolved Laser-Induced Fluorescence (LIF) techniques to conduct experimental lifetime measurements on Ti I (Salih & Lawler, 1990; Lawler, 1991; Lowe & Hannaford, 1991; Rudolph & Helbig, 1982)[18][19]

Recent Years: Advances in Experimental Techniques

In recent years, substantial advancements have been made in experimental techniques for studying titanium's atomic properties, particularly in the higher stages of ionization. Today, experimental results are available for every stage of titanium's ionization. These advancements have been driven by the need to interpret new spectroscopic observations of the sun at shorter wavelengths obtained from rocket- and satellite-borne spectrographs. These observations necessitated more energetic light sources for accurate analysis.

2. 2 For Ti II

1930s: Initial Understanding of Titanium (Ti) in Stellar Spectra

Titanium (Ti), a lighter element in the iron-group, garnered attention for its singly ionized state, Ti II, known for its abundant spectral lines observed in the ultraviolet, visible, and near-infrared spectra of B, A, and F stars. These lines were also observed in stellar winds, as reported by Hartman et al. in 2004 [20]

2000: Precise Oscillator Strengths for Ti I

Nilsson et al. (2000)[21] conducted a comprehensive investigation aiming to provide precise oscillator strength data for 44 transitions within titanium ion Ti I. Employing the time-resolved laser-induced fluorescence (TR-LIF) technique, they meticulously measured oscillator strengths spanning a wavelength range from 300 to 800 nm. The study compared these experimental results with existing theoretical and experimental data, providing valuable tables with measured oscillator strengths, uncertainties, and robust references. Additionally, the authors compiled energy levels and lifetimes for Ti I, encompassing various multiplets, and offered recommendations for future measurements, making this study a vital reference in atomic physics, astrophysics, and spectroscopy.

2008: Radiative Lifetimes of Ti II

Radiative lifetimes for 33 metastable states of Ti II were determined through a combination of experimental and theoretical approaches, using the pseudo-relativistic Hartree–Fock (HFR)

method by Cowan, as reported by Palmeri et al. in 2008[22]. This method effectively accounted for valence–valence and core–valence correlations.

1980s-1990s: Diverse Methods for Ti II Properties

Researchers employed various techniques to explore Ti II's properties. Kwiatkowski et al. (1985)[23] utilized laser-induced fluorescence (LIF) to measure lifetimes for 18 levels of Ti II. Bizzarri et al. (1993)[24] used time-resolved LIF on a slow Ti ion beam to assess lifetimes for 42 Ti II levels, useful for calculating transition probabilities for 100 emission lines. Similarly, Langhans et al. (1995)[25] used LIF to determine radiative lifetimes for 66 Ti II levels.

Roberts et al. (1973) [26]employed beam-foil techniques to calculate lifetimes for specific Ti II levels. Pickering et al. (2001)[27] and Wood et al. (2013)[28] harnessed Fourier transform spectroscopy to measure oscillator strengths, transition probabilities, and lifetimes for specific Ti II levels.

2001-2006: Advanced Methods and Computation

Wiese et al. (2001) [29]conducted high-sensitivity absorption spectroscopy experiments to measure oscillator strengths for vacuum ultraviolet resonance transitions within Ti II. Luke (1999)[30] employed a configuration interaction method to calculate transition rates between selected Ti II levels. Bautista et al. (2006) [31]used the AUTOSTRUCTURE code to compute transition rates and lifetimes for Ti II levels characterized by specific configurations.

2016-2020: Advanced Techniques for Higher-Excitation States

Lundberg et al. (2016)[32] utilized laser-induced fluorescence and Cowan's pseudo-relativistic Hartree–Fock method to calculate oscillator strengths, transition probabilities, and lifetimes for higher-excitation states of Ti II, accommodating core-polarization effects. Finally, Li et al. (2020)[33] employed the multiconfiguration Dirac–Hartree–Fock and relativistic configuration interaction methods (GRASP2018) to compute energy levels, oscillator strengths, and lifetimes for singly ionized titanium.

Within the scope of our thesis, our primary focus will be on the investigation of energy level configurations, transition probabilities, and the lifetimes of both Titanium I (Ti I) and Titanium II (Ti II) ions. This study aims to contribute to the field by providing a detailed comparative assessment, aligning our research findings with the established values available in the National Institute of Standards and Technology (NIST) database or experimental data available in the literature. This comprehensive analysis will offer valuable insights into the accuracy and reliability of our collected data, thus enhancing the understanding of these critical atomic properties.

Chapter 3

Quantum Mechanical Framework for Atomic Systems

3. 1 Single electron system

The Schrödinger equation is a fundamental equation in quantum mechanics that describes the behavior of a quantum system. It can be applied to different types of systems, such as single electron systems or multi electron systems.

A single electron system is a system that contains only one electron, such as a hydrogen atom or an ionized helium atom. The Schrödinger equation for a single electron system in one dimension is:

$$H\psi = E\psi \tag{3.1}$$

$$\frac{-\hbar^2}{2m}\frac{d^2\psi}{dx^2} + V(x)\psi = E\psi \tag{3.2}$$

where $\hbar$ is the reduced Planck constant, m is the mass of the electron, ψ is the wave function of the electron, $V(x)$ is the potential energy function, and E is the total energy of the system. The wave function ψ contains all the information about the quantum state of the electron, such as its position, momentum, and spin

3. 2 Multi-electron atomic systems

The description of a multi-electron atomic system presents significantly greater complexity compared to the treatment of hydrogen, primarily due to the presence of multiple electrons interacting within the atomic framework. In the case of hydrogen, the Hamiltonian operator for a

single electron encompasses only one potential term, which corresponds to the electron-nucleus Coulomb attraction potential denoted as V(r).

However, when extending the quantum mechanical treatment to a system with multiple electrons, several critical considerations come into play:

i. **Incorporating One-Electron Operators:** Firstly, it becomes necessary to account for all individual one-electron operators. These operators encompass the kinetic energy of each electron as it moves within the atomic system, as well as the attractive potential arising from the electron-nucleus interaction. The summation of these one-electron operators ensures a comprehensive representation of the system's behavior.

ii. **Incorporating Two-Electron Coulomb Repulsion Operators**: Additionally, the complexity escalates as the quantum description necessitates the inclusion of two-electron Coulomb repulsion operators. These operators account for the electrostatic repulsion that arises when two electrons within the atomic system approach each other, which constitutes a substantial interaction term.

For instance, the Helium atom or ions with helium-like electron configurations serve as pertinent examples where these considerations culminate in the formulation of the two-electron Hamiltonian operator. This operator encapsulates the intricate interplay of kinetic energies, electron-nucleus attraction potentials, and the Coulombic repulsion between electron pairs.

Schrodinger equation for multi-electron system can be written as:

$$H\psi = E\psi$$

Where,

$$H = \frac{p_1^2}{2m} + \frac{p_2^2}{2m} - \frac{e^2 Z}{r_1} - \frac{e^2 Z}{r_2} + \frac{e^2}{|\boldsymbol{r}_1 - \boldsymbol{r}_2|} \tag{3.3}$$

with the two electrons in positions $\boldsymbol{r}_1$ and $\boldsymbol{r}_2$.

The multi-electron Hamiltonian, reduced to number equations with atomic units (Ry),

And $H = H0 + H1$

$$H_0 = \sum_{i=1}^{N} \left[-\nabla_i^2 - \frac{2Z}{r_i} \right] \tag{3.4}$$

$$H_1 = \sum_{j<i} \frac{2}{r_{ij}} \tag{3.5}$$

which accounts for the two-electron Coulomb interaction. It becomes evident that beyond the scenario of a single electron, a direct solution Ψ from the Schrödinger equation is no longer feasible. In such cases, the approach necessitates the initiation with a trial function Ψ^{t}, typically represented parametrically. A prominent instance of this approach, employed in single-particle expansions, is the utilization of Slater-type orbitals denoted as $P_{nl}^{STO}(r)$. However, merely having a trial function is insufficient; it is imperative to establish constraints on the parameters within this function to ensure its usefulness.

This crucial prescription is known as the variational principle, a fundamental concept in quantum mechanics. The well-established Rayleigh–Ritz variational principle is a cornerstone in this context, as it sets an upper limit on the eigenvalue derived from the Schrödinger equation when employing a trial function. When applied specifically to the many-electron Hamiltonian, as discussed previously and as embodied in the Hartree–Fock scheme elaborated upon in the subsequent section, this leads to the formulation of the Hartree–Fock variational principle:

$$\delta\langle\Psi|H|\Psi\rangle = 0 \tag{3.6}$$

with sol^{n} $E=E_{min}$, notably because the spectrum of the non-relativistic Hamiltonian is bounded from below.

The Hartree–Fock variational principle plays a pivotal role in the study of many-electron systems, facilitating the determination of energetically favorable electronic configurations within complex atomic and molecular systems, taking into account the intricate interplay of electron-electron interactions and electron-nucleus interactions. This principle serves as a cornerstone in computational quantum chemistry, aiding in the prediction of molecular structures and properties with significant scientific and practical applications.

3. 3 The Hartree–Fock method

In the realm of quantum mechanics, when dealing with systems comprising multiple electrons under non-relativistic conditions, an analytical solution to the associated Hamiltonian becomes an unattainable pursuit. Instead, the Schrödinger equation is supplanted by the variational equation (Eq.3.6). The dominant and widely adopted methodology at the core of most quantum mechanical treatments in this context is the Hartree–Fock method. Commencing with a comprehensive set of integro-differential equations, the trial functions within this framework iteratively approach the elusive 'true' solution. It is important to note that these iterations are bound by the finite number of configurations specified for the functions.

The numerical instantiation of this approach adheres to the pioneering work of Hartree, who established a self-consistent iterative procedure for the determination of interelectron potentials and electronic wavefunctions [34]. Nevertheless, it's worth highlighting that the original Hartree method lacked the incorporation of electron exchange effects. This deficiency was rectified by

Fock[35], who expanded upon the methodology by introducing wavefunction antisymmetrization, thereby accounting for electron exchange effects in an ab-initio fashion. This iterative framework, augmented by the inclusion of electron exchange, is formally known as the self-consistent Hartree–Fock method [34].

We initiate our investigation using the exact Hamiltonian expressed as a Rydberg–Bohr scaled number equation, specifically referencing Equations (3.4) and (3.5)

$$H = \sum_{i=1}^{N} \left[-\nabla_i^2 - \frac{2Z}{r_i} \right] + \sum_{j \neq i} \frac{2}{r_{ij}} \tag{3.7}$$

we also define the concise notation for the one-electron operator,

$$f_i \equiv -\nabla_i^2 - \frac{2Z}{r_i} \tag{3.8}$$

representing the kinetic energy term $p^2/2m$ and the nuclear potential, as well as the two-electron operator,

$$g_{ij} \equiv \frac{2}{r_{ij}} \tag{3.9}$$

Then the Rydberg–Bohr scaled Hamiltonian becomes,

$$H = \sum_{i} f_i + \sum_{j \neq i} g_{ij} \equiv F + G \tag{3.10}$$

Here, F and G represent interaction operators encompassing all electrons within the atom. It is important to note that the electron-electron interaction, in conjunction with the electron-nuclear interaction, collectively transforms the non-hydrogenic atom into a many-body problem that cannot be solved exactly. In the Schrödinger equation for hydrogen, where the Coulomb potential is traditionally represented as $2Z/r$, a potential $V(r)$ must be introduced. This potential, $V(r)$, is designed to accommodate the individual electron wavefunctions $\psi(r, \vartheta, \phi, m_s)$. The wavefunction ψ is expressed as a spin-orbital, which is a product of a spatial coordinate function $\varphi(r)$ and a spin function ζ_{m_s}, with spin components ±1/2.

$$\psi_{n,l,m_l,m_s}(r,\vartheta,\varphi,m_s) = \varphi(\boldsymbol{r})\zeta_{m_s} \tag{3.11}$$

In our analysis, we introduce a formalism to represent the spin-orbital by substituting spatial coordinates with quantum numbers,

$\psi_{n,l,m_l,m_s} = \varphi(nlm_l)\zeta\,(m_s)$. It's essential to recognize that within the electron configuration of the atom, each electron is influenced by the collective potential generated by all other electrons. Consequently, a pivotal challenge lies in constructing the potential, $V(r_i)$, from the set of all ψ_i specific to the *i*-th electron in a self-consistent manner. This objective underpins the core of the self-consistent iterative methodology applied in solving the Hartree–Fock equations.

Furthermore, the individual electronic states ψ_i play a crucial role in the assembly of the comprehensive atomic wavefunction for a given state within the multi-electron atom. Assuming the atom constitutes an N-electron system, the total atomic wavefunction manifests as the product of individual one-electron spin-orbitals.

$$\boldsymbol{\psi_{n,l,m_l,m_s}(r,\theta,\phi,m_s) = \prod_{i=1}^{N}\psi_{n_i,\ell_i,m_{\ell_i},m_{s_i}} = \left(\psi_{n_1,l_1,m_{l_1},m_{s_1}}\right)\left(\psi_{n_2,l_2,m_{l_2},m_{s_2}}\right)\ldots\left(\psi_{n_N,\ell_N,m_{\ell_N},m_{s_N}}\right)}} \quad (\mathbf{3.12})$$

However, a straightforward product representation of the total wavefunction falls short in accounting for electron exchange, a crucial aspect that necessitates the interchange of electronic coordinates to adhere to the general antisymmetry postulate. The wavefunction must undergo a change in sign upon the exchange of coordinates between any two electrons, whether in terms of their spatial or spin properties.

The Hartree–Fock description of a multi-electron system integrates the essential antisymmetrization aspect into the wavefunction representation. To illustrate this, let's consider the example of the Helium atom. The mathematical formulation of a two-particle antisymmetric wavefunction can be expressed as:

$$\Psi(1,2) = \frac{1}{\sqrt{2}}[\psi_1(1)\psi_2(2) - \psi_1(2)\psi_2(1)] \tag{3.13}$$

Indeed, this representation corresponds to the standard expansion of the determinant of a

2×2 matrix, with its elements associated with the two electrons and their respective coordinates. In mathematical terms, it can be expressed as follows:

$$\Psi = \frac{1}{\sqrt{2}} \begin{vmatrix} \psi_1(1) & \psi_1(2) \\ \psi_2(1) & \psi_2(2) \end{vmatrix} \tag{3.14}$$

The concept of antisymmetry becomes evident in this context. The interchange of coordinates 1 and 2 results in a change in the sign of the determinant, as expressed in (Eq. 3.14). However, it's crucial to note that when both coordinates of the two electrons become identical, the corresponding quantum state cannot exist. This is because the antisymmetric wavefunction described in (Eq. 3.14) would possess two identical rows or columns, leading to a determinant value of zero.

In helium-like two-electron systems, the average potential energy of electron 1 in the field of electron 2 is described as:

$$U_1(r_1) = \int \psi^*(\boldsymbol{r}_2) \frac{2}{r_{12}} \psi(\boldsymbol{r}_2) \mathrm{d}\boldsymbol{r}_2 \tag{3.15}$$

Similarly, we can express the potential energy of electron 2 within the influence of electron 1. With this consideration, we introduce the definition of an effective one-electron Hamiltonian operator as:

$$H_i = \frac{p_i^2}{2m} - \frac{e^2 Z}{r_i} + U_i(r_i). \tag{3.16}$$

In correspondence to the Schrödinger equation applied to each individual electron, we establish the following equations:

$$H_1(\boldsymbol{r}_1)\psi(\boldsymbol{r}_1) = \epsilon_1\psi(\boldsymbol{r}_1)$$
$$H_2(\boldsymbol{r}_2)\psi(\boldsymbol{r}_2) = \epsilon_2\psi(\boldsymbol{r}_2). \quad (3.17)$$

Here,

- $\psi(\boldsymbol{r}_1)$ and $\psi(\boldsymbol{r}_2)$ are the wavefunctions associated with electrons 1 and 2.
- $H_1(\boldsymbol{r}_1)$ and $H_2(\boldsymbol{r}_2)$ represent the Hamiltonian operators for electrons 1 and 2, respectively.
- ϵ_1 and ϵ_2 denote the eigenvalues corresponding to electrons 1 and 2, respectively.

The Hartree–Fock equations for a system consisting of two electrons are presented herein. These equations exhibit coupling with respect to the radial distance 'r' (r-dependence), as well as spin dependence, which arises due to the exchange effect. However, the explicit expression of spin dependence is not provided in the preceding equations.

The operator $H_1(\boldsymbol{r}_1)$ is intrinsically dependent on the electron wave function $\psi(\boldsymbol{r}_2)$. Consequently, to solve $H_1(\boldsymbol{r}_1)$, it becomes imperative to have knowledge of $\psi(\boldsymbol{r}_2)$. To address this, a preliminary or trial electron wave function $\psi(\boldsymbol{r}_2)$ is initially adopted, and it is utilized to derive the electron wave function $\psi(\boldsymbol{r}_1)$in accordance with the variational criterion, as denoted by (Eq. 3.8).

Notably, owing to the identical forms of the wave functions $\psi(\boldsymbol{r}_1)$ and $\psi(\boldsymbol{r}_2)$ the updated wave function $\psi(\boldsymbol{r}_2)$ is subsequently employed to derive $\psi(\boldsymbol{r}_1)$ once more. This iterative process persists until the desired level of accuracy is achieved. This computational methodology is commonly referred to as the Hartree–Fock self-consistent field method, abbreviated as HF-SCF.

Drawing an analogy with the helium atom, we can represent the wave function for an N-electron system in the determinantal form as follows:

$$\Psi = \frac{1}{\sqrt{N!}} \begin{vmatrix} \psi_1(1) & \psi_1(2) & \dots & \psi_1(N) \\ \psi_2(1) & \psi_2(2) & \dots & \psi_2(N) \\ \dots & \dots & \dots & \dots \\ \psi_N(1) & \psi_N(2) & \dots & \psi_N(N) \end{vmatrix} \tag{3.18}$$

Equation (3.18) is referred to as the Slater determinant. Similar to the two-electron determinant (Eq. 3.14), when all coordinates of any two electrons coincide, it results in two identical rows or columns within the determinant, causing the determinant to become zero. This observation leads us to the immediate implication of the Pauli exclusion principle: no two electrons can possess identical spatial and spin quantum numbers simultaneously.

In the expression ψ_a, each subscript $'a'$ represents a set of four quantum numbers (n, l, m_l, m_s) while each variable $'i'$ corresponds to spatial coordinates $'r'$ and spin-coordinates in the position $'i'$ of electron $'a'$. It's noteworthy that a spin-orbital carries a parity factor of $(-1)^l$, and as a consequence, the Slater determinant possesses a well-defined parity, which is determined by $(-1)^{\sum_i l_i}$ across all particles. This parity can result in the Slater determinant being either even or odd under the inversion transformation, where r_i is transformed to $-r_i$, depending on whether the sum $\sum_i l_i$ is even or odd.

The calculations of atomic structure follow the initial prescription outlined by Hartree, which involves the development of a self-consistent iterative procedure for determining both the inter-electron potentials and the electronic wavefunctions [34]. It is worth noting that the original Hartree method lacked consideration for the electron exchange effect. To address this limitation, the self-consistent Hartree-Fock method was introduced, which also employs an iterative scheme [34]–[36].

In the context of atomic wavefunctions, characterized by a set of quantum numbers (nl), the atomic wavefunction can be expressed as a composition of individual spin-orbital wavefunctions, denoted as $\psi_{nl} = \varphi(n_l m_l)\zeta(m_s)$. Here, ψ_{nl} represents the atomic wavefunction for a specific electronic configuration with quantum numbers (nl).

Moreover, it is crucial to acknowledge that the wavefunctions $\psi_a(j)$ are subject to the orthonormality condition, ensuring that they are properly normalized and orthogonal to each other, a fundamental requirement in quantum mechanics.

$$\langle \psi_a(j)\psi_b(j)\rangle = \delta_{ab} \tag{3.19}$$

It's worth noting that the Hartree-Fock variational principle implies that the chosen wavefunction corresponds to the ground state energy

$$E_0 \leq E[\Psi] = \langle \Psi|H|\Psi\rangle \tag{3.20}$$

In the Hartree-Fock method, the initial trial wavefunction is a Slater determinant. This substitution of the wavefunction determinant leads to the introduction of one-operator terms, involving one-electron functions, and two-operator integrals, much like in the case of helium. The expectation value of the one-electron or one-body term can be readily evaluated as

$$\langle \Psi|H_0|\Psi\rangle = \sum_k \langle \psi_k(i)|H_0|\psi_k(i)\rangle = \sum_k I_k \tag{3.21}$$

H1 represents the sum of two-electron or two-body operators, which can be expressed as follows:

$$\langle \Psi|H_1|\Psi\rangle = \sum_{k,l\neq k} \left[\left\langle \psi_k(i)\psi_l(j)\left|\frac{2}{r_{ij}}\right|\psi_k(i)\psi_l(j)\right\rangle - \left\langle \psi_k(i)\psi_l(j)\left|\frac{1}{r_{ij}}\right|\psi_l(i)\psi_k(j)\right\rangle\right] \tag{3.22}$$

summing over all $N(N\ -\ 1)/2$ pairs of orbitals. We can also write it as

$$\langle \Psi|H_1|\Psi\rangle = \frac{1}{2}\sum_k \sum_l \left[\left\langle \psi_k(i)\psi_l(j)\left|\frac{2}{r_{ij}}\right|\psi_k(i)\psi_l(j)\right\rangle - \left\langle \psi_k(i)\psi_l(j)\left|\frac{1}{r_{ij}}\right|\psi_l(i)\psi_k(j)\right\rangle\right] \tag{3.23}$$

Here the first term is called direct term

$$J_{kl} = \left\langle \psi_k(i)\psi_l(j) \left| \frac{1}{r_{ij}} \right| \psi_k(i)\psi_l(j) \right\rangle \tag{3.24}$$

This expression represents the average value of the interaction $1/r_{ij}$ relative to $\psi_k(i)\psi l_l(j)$. The second term is commonly referred to as the exchange term

$$K_{kl} = \left\langle \psi_k(i)\psi_l(j) \left| \frac{1}{r_{ij}} \right| \psi_l(i)\psi_k(j) \right\rangle \tag{3.25}$$

This term represents the matrix element of the interaction, specifically $1/r_{ij}$ between two quantum states, $\psi_k(i)\psi_l(j)$ and $\psi_l(i)\psi_k(j)$, which results from the interchange of electrons within the system . Hence total energy is

$$E[\Psi] = \sum_i I_i + \frac{1}{2}\sum_i \sum_j \left[J_{ij} - K_{ij}\right] \tag{3.26}$$

E should be stationary with respect to the variations of the spin-orbitals; ψ_i subject to N^2 orthonormality conditions. Hence the variational principle introduces N^2 Lagrange multipliers (or variational parameters) λ_{kl}, such that (incorporating the orthonormal conditions)

$$\delta E - \sum_k \sum_l \lambda_{kl}\, \delta\langle \psi_k \mid \psi_l \rangle = 0 \tag{3.27}$$

From the above equation it is seen that $\lambda_{kl} = \lambda_{kl}^*$ and hence N^2 Lagrange multipliers may be considered as the elements of a Hermitian matrix. Any Hermitian matrix can be diagonalized by a unitary transformation. Hence, we can assume that the matrix of Lagrange multipler λ_{kl} is diagonal with elements $E_k\delta_{kl}$, that is,

$$\delta E - \sum_k E_k\, \delta\langle \psi_k \mid \psi_k \rangle = 0 \tag{3.28}$$

Varying the Schrödinger equation with respect to spin-orbitals ψ_i and using the above relations, we can find, for the N spin-orbitals, the set of integro-differential equations

$$\left[-\nabla_i^2 - \frac{2Z}{r_i}\right]\psi_k(i) + \left[\sum_l \int \psi_l^*(j)\frac{2}{r_{ij}}\psi_l(j)\mathrm{d}j\right]\psi_k(i) - \sum_l \left[\int \psi_l^*(j)\frac{2}{r_{ij}}\psi_k(j)\mathrm{d}j\right]\psi_l(i) = E_k\psi_k(i) \tag{3.29}$$

where the summation over k extends over the N occupied spin-orbitals, and the integral $\int \ldots \mathrm{d}j$ implies an integration over the spatial coordinates r and a summation over the spin-coordinate of electron j. These equations are the Hartree-Fock equations of a multi-electron system. We can separate the spin functions from the spin-orbital by writing $\psi_k(i) = u_k(r_i)\chi_{1/2,m_l^k}$ and using the orthonormality condition $\left\langle \chi_{1/2,m_l^k}\chi_{1/2,m_l^j}\right\rangle = \delta_{m_L^k,m_L^j}$. Then the Hartree-Fock equations are in a form that involves only the spatial part,

$$\left[-\nabla_i^2 - \frac{2Z}{r_i}\right]u_k(\boldsymbol{r}_i) + \left[\sum_l \int u_l^*(\boldsymbol{r}_j)\frac{2}{r_{ij}}u_l(\boldsymbol{r}_j)\mathrm{d}\boldsymbol{r}_j\right]u_k(\boldsymbol{r}_i) - \sum_l \delta_{m_L^k,m_L^l}\left[\int u_l^*(\boldsymbol{r}_j)\frac{2}{r_{ij}}u_k(\boldsymbol{r}_j)\mathrm{d}\boldsymbol{r}_j\right]u_l(\boldsymbol{r}_i) = E_k u_k(\boldsymbol{r}_i) \tag{3.30}$$

The integrals are frequently represented in terms of direct and exchange operators. Specifically, the direct operator V_l^d is defined as:

$$V_l^d(\boldsymbol{r}_i) = \int u_l^*(\boldsymbol{r}_j)\frac{1}{\boldsymbol{r}_{ij}}u_l(\boldsymbol{r}_j)d\boldsymbol{r}_{\boldsymbol{j}} \tag{3.31}$$

which represents the electrostatic repulsion potential due to electron j, averaged over the orbital u_l. In addition to the direct operator, there is the non-local exchange operator, which is defined as:

$$V_l^{\mathrm{ex}}(\boldsymbol{r}_i)\psi(i) = \delta_{m_L^k,m_L^l}\left[\int u_l^*(\boldsymbol{r}_j)\frac{1}{r_{ij}}u_k(\boldsymbol{r}_j)d\boldsymbol{r}_j\right] \times u_l(\boldsymbol{r}_i)\chi_{\frac{1}{2},m_L^l} = \delta_{m_L^k,m_L^l}V_l^{\mathrm{ex}}(\boldsymbol{r}_i)\chi_{\frac{1}{2},m_L^l} \tag{3.32}$$

$V_l^{\text{ex}}(\boldsymbol{r}_i)$ acts on the spatial coordinates only. The Hartree-Fock equation (Eq. 3.31) for a given spin-orbital for electron i may be written in terms of the one- and two-electron operators f_i and g_{ij} defined in (Eq. 3.24) and (Eq. 3.25)

$$\begin{aligned} f_i\psi_i(1) + \left[\sum_{j\neq i} \int \psi_j^*(2) g_{12} \psi_j(2) \mathrm{d}V\right]\psi_i(1) \\ -\sum_{j\neq i}\left[\int \psi_j^*(2) g_{12}\psi_i(2)\mathrm{d}V\right]\psi_j(1) = \epsilon_i\psi_i(1) \end{aligned} \tag{3.33}$$

Several important physical aspects of these equations merit attention.

- Firstly, the two-electron integration variable, denoted as dV, encompasses all spatial and spin coordinates, succinctly represented as (1) and (2).
- Secondly, it's crucial to acknowledge that the summation for each electron i inherently involves interactions with all other electrons, with the exception of itself, as is self-evident.
- Thirdly, the second term on the left side of the equation represents the repulsive Coulomb interaction between electron i and electron j. In contrast, the third term on the left side is referred to as the "exchange term," a concept without a classical analogue. Nonetheless, the exchange effect is a physical phenomenon intricately linked to the spin of the electron: two electrons sharing the same spin quantum number $\zeta(m_s)$ cannot simultaneously occupy the same spatial position $\boldsymbol{r}$.
- Furthermore, the two integrals featured on the left side of the equation are denoted as the "direct integral" J (as per Eq. 3.24) and the "exchange integral" K (as per Eq. 3.25) which can also be expressed as:

$$\begin{aligned} J_j(1)\psi_i(1) &= \left[\int \psi_j^*(2) g_{12}\psi_j(2)\mathrm{d}V\right]\psi_i(1) \\ K_j(1)\psi_j(1) &= \left[\int \psi_j^*(2) g_{12}\psi_i(2)\mathrm{d}V\right]\psi_j(1) \end{aligned} \tag{3.34}$$

Note the interchange of i and j in the K-integral with respect to the J-integral. In the next chapter, we shall make use of these integrals to express the matrix elements.

3. 4 Central field approximation for a multi-electron system

Calculations of wavefunctions and energies within the Hartree-Fock approximation were historically challenging until the advent of powerful computers. In many cases, and even today, the central field approximation has been widely employed to mitigate these difficulties. The central field approximation helps simplify the treatment of electron-electron interactions.

Specifically:

- The term H_1 in the context of the Hartree-Fock approximation contains non-central forces between electrons, including a significant spherically symmetric component.

- In this approach, it is assumed that each electron experiences the average charge distribution resulting from the presence of all other electrons. To model this, a potential energy function $V(r_i)$ is constructed using a one-electron operator and is a good approximation to the actual potential of the *i* th electron in the field of the nucleus and the other $N-1$ electrons. When these contributions are summed over all electrons, the resulting charge distribution is spherically symmetric. This approximation serves as a reasonably accurate representation of the actual potential energy.

- The effective potential experienced by each electron due to electron–nuclear attraction and electron–electron repulsion, in H_0 and H_1 respectively, consists of a radial and a non-radial part. The central-field approximation involves neglecting the non-radial part, while retaining the radial part assumed to be dominant. Unlike the Hartree–Fock method, where we explicitly account for the electron–electron interaction, we now seek an effective potential $U(r)$ which combines the radial electron– nuclear term Ze^2/r_i with an averaged radial component of the electron–electron term. The approximate N -electron Hamiltonian then becomes

$$H = -\sum_{i=1}^{N} \frac{\hbar^2}{2m}\nabla_i^2 + U(r) \tag{3.35}$$

Where,

$$U(r) = -\sum_{i=1}^{N} \frac{e^2 Z}{r_i} + \left\langle \sum_{i \neq j}^{N} \frac{e^2}{r_{ij}} \right\rangle \tag{3.36}$$

$U(r)$ is central field potential. at first sight, it should be noticed that $U(r)$ contains the electron–nuclear potential term Z/r, which increases in magnitude with Z. Therefore, for a given number of electrons N the central-field approximation improves in accuracy with increasing charge $z \equiv (Z - N + 1)$ of an ion, or along an isoelectronic sequence. First, we note that the boundary conditions on $U(r)$ are

$$U(r) = \begin{cases} -\frac{Z}{r}, & r \to 0 \\ -\frac{z}{r}, & x \to \infty \end{cases} \tag{3.37}$$

3. 5 Thomas–Fermi–Dirac approximation

A notably valuable approach in the realm of atomic physics is the Thomas-Fermi-Dirac-Amaldi (TFDA) model [37]. This model offers an effective framework by making the assumption of spherically symmetric charge distribution. Its precursor, the Thomas-Fermi model, characterized atomic electrons as a degenerate Fermion gas governed by the relationship between electron density and the maximum momentum, known as the Fermi momentum (p_F). According to this model, electrons are considered to occupy cells in phase space, each with a volume of h^3, accommodating two electrons—one with spin up and the other with spin down. These cells are entirely filled up to a maximum Fermi momentum of (p_F). Consequently, the spatial electron density can be described as:

$$\rho = \frac{\frac{4}{3}\pi p_F^3}{\frac{h^3}{2}} \tag{3.38}$$

An enhancement over the Thomas-Fermi model is achieved by incorporating a simplified treatment of the electron-electron exchange effect. In the presence of electron-electron exchange, electrons with the same spin exhibit spatial avoidance—a crucial requirement dictated by the antisymmetry principle, fundamental for the existence of the electron system.

Leveraging principles of quantum statistics, the Thomas-Fermi-Dirac-Amaldi (TFDA) model introduces a continuous function $\boldsymbol{\varphi}(\boldsymbol{x})$ that satisfies:

$$U(r) = \frac{Z_{\text{eff}}(\lambda_{nl}, r)}{r} = -\frac{Z}{r}\phi(x), \tag{3.39}$$

Where,

$$\phi(x) = \mathrm{e}^{-\frac{Zr}{2}} + \lambda_{nl}\left(1 - \mathrm{e}^{-\frac{Zr}{2}}\right),\ x = \frac{r}{\mu}, \tag{3.40}$$

and μ is a constant:

$$\mu = 0.8853\left(\frac{N}{N-1}\right)^{\frac{2}{3}} Z^{-\frac{1}{3}} \tag{3.41}$$

The function $\phi(x)$ is a solution of the potential equation

$$\frac{\mathrm{d}^2\phi(x)}{\mathrm{d}x^2} = \frac{1}{\sqrt{x}}\phi(x)^{\frac{3}{2}} \tag{3.42}$$

From (Eq. 3.37) the boundary conditions on $\phi(x)$ are

$$\phi(0) = 1,\ \phi(\infty) = -\frac{Z-N+1}{Z} \tag{3.43}$$

Having determined a central potential $U(r)$, for example as in the TFDA approximation above, we compute the one-electron orbitals $P_{nl}(r)$ by solving the wave equation

$$\left[\frac{\mathrm{d}^2}{\mathrm{d}r^2} - \frac{l(l+1)}{r^2} + 2U(r) + \epsilon_{nl}\right] P_{nl}(r) = 0 \tag{3.44}$$

This is similar to the radial equation for the hydrogenic case, with the same boundary conditions on $P_{nl}(r)$ as $r \to 0$ and $r \to \infty$, and $(n - l + 1)$ nodes. The secondorder radial differential equation is solved numerically since, unlike the hydrogenic case, there is no general analytic solution. Equation 2.125 may be solved by both inward and outward integration, matching the two solutions at a suitable point. As $r \to 0$, the outward solution is given by the first few points of a power series expansion. The inward solution begins from the asymptotic region $r \to \infty$, using an exponentially decaying function appropriate for a bound state, such as the normalized Whittaker function,

$$W(r) = \mathrm{e}^{-\frac{zr}{v}} \left(\frac{2zr}{v}\right) \left(1 + \sum_{k=1}^{\infty} \frac{a_k}{r^k}\right) \mathcal{N} \tag{3.45}$$

where $v = \frac{z}{\sqrt{\epsilon}}$ is the effective quantum number (and as such not necessarily an integer) and ϵ is the eigenvalue. The coefficients are

$$a_1 = v\{l(l+1) - v(v-1)\} \frac{1}{2z} \tag{3.46}$$

$$a_k = a_{k-1} v\{l(l+1) - (v-k)(v-k+1)\} \frac{1}{2kz} \tag{3.47}$$

and the normalization factor is

$$\mathcal{N} = \left\{\frac{v^2}{z} \Gamma(v + l + 1) \Gamma(v - 1)\right\}^{-\frac{1}{2}} \tag{3.48}$$

The one-electron spin-orbital functions then assume the familiar hydrogenic form familiar hydrogenic form

$$\begin{aligned} \psi_{n,\ell,m_\ell,m_s}(r,\theta,\phi,m_s) &= \phi(r,\theta,\phi)\zeta_{m_s} \\ &= R_{n\ell}(r)\mathrm{Y}_{\ell,m_\ell}(\theta,\phi)\zeta_{m_s} \\ &= \frac{P_{n\ell}(r)}{r}\mathrm{Y}_{\ell,m_\ell}\zeta_{m_s}. \end{aligned} \tag{3.49}$$

The TFDA one-electron orbitals are determined through statistical treatment applied to a free-electron gas. However, this approach overlooks the inherent shell structure that is a fundamental aspect of the Hartree-Fock method, where electron-electron interactions give rise to distinct electron shells.

3. 6 Relativistic Breit-Pauli Approximation

The relativistic Breit-Pauli approximation is a method of accounting for some of the relativistic effects in the electronic structure of multi-electron systems, such as atoms and molecules. It is based on the expansion of the relativistic Hamiltonian in powers of the fine-structure constant α which is a measure of the strength of the electromagnetic interaction. The Breit-Pauli approximation includes the terms up to the order of α^2 which are the most important for low-energy phenomena.

The necessity of the relativistic Breit-Pauli approximation for treating multi-electron systems arises from the fact that the non-relativistic Schrödinger equation does not capture all the physical features of the quantum systems, such as the spin-orbit coupling, the Darwin term, and the mass-velocity correction. These effects can have significant influences on the energy levels, transition probabilities, and magnetic properties of the systems, especially for heavy elements or high angular momentum states.

Key features of the relativistic Breit-Pauli approximation include:

- **Incorporation of Special Relativity:** Special relativity becomes significant when the speed of electrons approaches a significant fraction of the speed of light (c). This can occur in heavy atoms with high nuclear charge or in highly excited states. The Breit-Pauli approximation accounts for relativistic effects, such as the relativistic increase in electron mass and the correction to the electron kinetic energy due to its velocity.
- **Spin-Orbit Interaction:** The Breit-Pauli approximation includes the spin-orbit interaction, which arises from the relativistic correction to the electron's kinetic energy. This interaction couples the electron's orbital angular momentum with its intrinsic spin angular momentum, leading to fine structure splitting in atomic spectra.

- **Darwin Term:** This term accounts for the relativistic correction to the electron's kinetic energy due to the spatial variation of the electrostatic potential around the nucleus. It contributes to the Lamb shift in atomic spectra.
- **Breit Interaction:** The Breit interaction is a relativistic correction to the electron-electron interaction potential. It includes terms that account for the finite speed of electromagnetic interactions and the magnetic interaction between electrons. These corrections are typically small but become important in heavy atoms.

For a multi-electron system, the relativistic Breit-Pauli equation is:

$$H_{BP}\psi = [H_{NR} + H_{mass} + H_{Dar} + H_{so} + \frac{1}{2}\sum_{i\neq j}^{N}\left[g_{ij}(\boldsymbol{so} + \boldsymbol{so'}) + g_{ij}(ss') + g_{ij}(css') + g_{ij}(d) + g_{ij}(\boldsymbol{oo'})\right]]\psi \quad (3.50)$$

where the non-relativistic Hamiltonian is

$$H_{NR} = \left[\sum_{i=1}^{N}\left\{-\nabla_i^2 - \frac{2Z}{r_i} + \sum_{j>i}^{N}\frac{2}{r_{ij}}\right\}\right] \quad (3.51)$$

the Breit interaction is

$$H_B = \sum_{i>j}\left[g_{ij}(so + so') + g_{ij}(ss')\right] \quad (3.52)$$

and one-body correction terms are

$$H_{mass} = -\frac{\alpha^2}{4}\sum_i p_i^4 \quad (3.53)$$

$$H_{Dar} = \frac{\alpha^2}{4}\sum_i \nabla^2\left(\frac{Z}{r_i}\right) \quad (3.54)$$

$$H_{so} = \frac{Ze^2\ h^2}{2\ m^2c^2r^3}\ L \cdot S \tag{3.55}$$

Here, H_{mass} , H_{Dar} , H_{so} are the relativistic mass-velocity correction, Darwin and spin–orbit terms. Spin-orbit interaction energy: $E_{SO} = \frac{1}{2}\ A\hbar^2[\ J(\ J+1) - L(L+1) - S(S+1)]$ where A is the fine structure splitting constant which is proportional to z as $A \propto \frac{z^4}{n^3}$ and separation between two fine structure levels is given by $\frac{1}{2}A\hbar^2 j$

Chapter 4

Atomic Radiative Processes and Transitions

4. 1 Radiative processes

Radiative processes are the physical phenomena of energy transfer in the form of electromagnetic radiation. They occur when a medium releases or absorbs energy by emitting or absorbing photons, which are the elementary particles of light. The propagation of radiation through a medium is affected by absorption, emission, and scattering processes. The equation of radiative transfer describes these interactions mathematically.

Radiative processes are important for understanding the spectra and the dynamics of various astrophysical and laboratory systems, such as stars, planets, nebulae, plasmas, lasers, and LEDs. They can provide information about the temperature, density, composition, structure, and evolution of these systems. They can also affect the energy balance, the chemical reactions, and the radiative feedback of these systems.

Below, we present an overview of several radiative processes

1. Photoexcitation and de-excitation

Photoexcitation and deexcitation are processes where an atom or a molecule absorbs or emits a photon and changes its energy state. The reaction can be written as:

$$A + h\nu \leftrightarrow A^*$$

where A is the atom or molecule in the ground state, A^* is the atom or molecule in the excited state, and $h\nu$ is the photon energy.

We need to study these processes because:

i. They are important for understanding the spectra and the dynamics of atomic and molecular systems, as well as their interactions with electromagnetic radiation.

ii. They can provide information about the energy levels, transition probabilities, and lifetimes of the excited states.

iii. They can affect the population distribution, the temperature, and the pressure of the systems.

2. Photoionization and radiative recombination

Photoionization and radiative recombination are processes where an atom or a molecule loses or gains an electron due to the absorption or emission of a photon. The reaction can be written as:

$$A + h\nu \leftrightarrow A^+ + e^-$$

where A is the atom or molecule in the neutral state, A^+ is the atom or molecule in the ionized state, e^- is the free electron, and $h\nu$ is the photon energy.

We need to study these processes because:

i. They are important for understanding the ionization and recombination rates of atomic and molecular systems, as well as their effects on the plasma properties and the radiation fields.

ii. They can provide information about the ionization potential, the recombination coefficient, and the photoionization cross section of the systems.

iii. They can affect the charge balance, the electron density, and the opacity of the systems.

3. Autoionization and dielectronic recombination

Autoionization and dielectronic recombination are processes where an atom or a molecule undergoes a transition between two bound states that involves the emission or absorption of an electron. The reaction can be written as:

$$A^* \leftrightarrow A + e^-$$

where A^* is the atom or molecule in a doubly excited state, A is the atom or molecule in a lower excited state, and e^- is the free electron.

We need to study these processes because:

i. They are important for understanding the resonance structures and the line shapes of atomic and molecular spectra, as well as their effects on the collisional processes and the radiative transfer.

ii. They can provide information about the resonance energies, widths, and positions of the doubly excited states.

iii. They can affect the recombination rates, the line intensities, and the line broadening of the systems.

4. Electron impact excitation

Electron impact excitation is a process where an atom or a molecule is excited by the collision with a free electron. The reaction can be written as:

$$A + e^- \rightarrow A^* + e^-$$

where A is the atom or molecule in the ground state, $A^*$is the atom or molecule in the excited state, and e^- is the free electron.

We need to study this process because:

i. It is important for understanding the excitation rates and the cross sections of atomic and molecular systems, as well as their effects on the plasma properties and the emission spectra.

ii. It can provide information about the collision strength, the excitation function, and the angular distribution of the scattered electrons.

iii. It can affect the population distribution, the temperature, and the pressure of the systems.

5. Electron impact ionization

Electron impact ionization is a process where an atom or a molecule is ionized by the collision with a free electron. The reaction can be written as:

$$A + e^- \rightarrow A^+ + 2e^-$$

where A is the atom or molecule in the neutral state, $A^+$is the atom or molecule in the ionized state, and $e^-$is the free electron.

We need to study this process because:

i. It is important for understanding the ionization rates and the cross sections of atomic and molecular systems, as well as their effects on the plasma properties and the radiation fields.

ii. It can provide information about the ionization potential, the ionization function, and the angular distribution of the ejected electrons.

iii. It can affect the charge balance, the electron density, and the opacity of the systems.

6. Hydrogen impact ionization

Hydrogen impact ionization is a process where an atom or a molecule is ionized by the collision with a hydrogen atom. The reaction can be written as:

$$A + H \rightarrow A^{+} + H + e^{-}$$

where A is the atom or molecule in the neutral state, $A^{+}$is the atom or molecule in the ionized state, H is the hydrogen atom, and e^{-} is the free electron.

We need to study this process because:

i. It is important for understanding the ionization rates and the cross sections of atomic and molecular systems in hydrogen-rich environments, such as interstellar clouds, stellar atmospheres, and planetary nebulae.

ii. It can provide information about the hydrogen impact ionization potential, the hydrogen impact ionization function, and the angular distribution of the ejected electrons and hydrogen atoms.

iii. It can affect the charge balance, the electron density, and the opacity of the systems.

4. 2 Photo Excitation and De-excitation

Radiative transitions in atoms involve electron movements between bound states. These transitions occur when an electron absorbs a photon, moving to a higher energy level (photo-excitation), or emits a photon, returning to a lower level (de-excitation or radiative decay). In atomic notation,

this is expressed as $X + h\nu \rightarrow X^*$ where X^*represents an excited state with finite lifetimes compared to the ground state.

These processes lead to absorption and emission lines in a spectrum, and their intensity depends on both atomic properties and external conditions. Understanding these qualitative and quantitative aspects is crucial for spectral analysis. Laboratory conditions for spectral formation can differ significantly from astrophysical conditions.

In astrophysics, transitions are categorized as 'allowed,' 'forbidden,' or 'intersystem.' 'Forbidden' lines are not impossible but have much lower transition rates than allowed lines, resulting in weaker observed lines. However, in astrophysical environments like H II regions, despite their low intrinsic probabilities, forbidden transitions can dominate due to specific physical conditions—low temperatures and densities.

The classification of radiative transitions relies on Einstein's coefficients A and B, which are determined by intrinsic atomic properties and can be computed quantum mechanically or measured in the laboratory. It's crucial to note that these coefficients are independent of external factors like temperature or density in the source, while the intensities of lines do depend on these extrinsic conditions.

Einstein's transition probabilities or rates are fundamental and do not consider external factors. We begin by explaining the basics of atomic transitions, particularly the formation of emission and absorption lines, in terms of the Einstein relations. This is followed by a first-order quantum mechanical treatment, typically suitable for astrophysical applications. While more advanced treatments, including quantum electrodynamic (QED) effects, exist for extreme precision, our focus here is on outlining the fundamental framework used in practical calculations.

When incident photons from the surrounding radiation field interact with atoms, various transitions can occur. Quantum mechanically, the probability of these transitions is computed using a transition matrix element. This matrix element depends on the wavefunctions of the initial and final states and an operator associated with the moment of the radiation field. These moments can be dipole moments for allowed transitions or higher-order multipoles for forbidden transitions. Additionally, the symmetries of the atomic states involved, as determined by the quantized angular

and spin momenta of these states, play a crucial role in governing radiative transitions. These rules, specifying the symmetries concerning a particular type of transition, are known as selection rules.

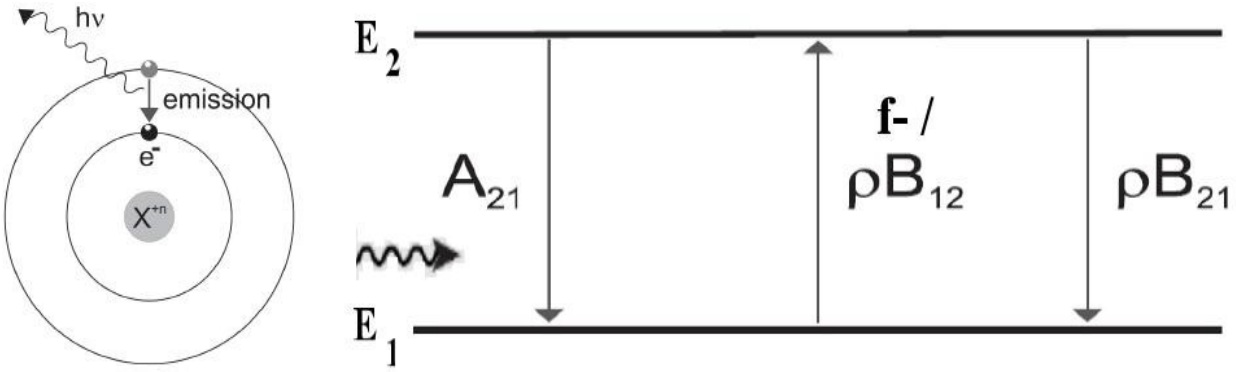

Figure 4.1:Electron impact excitation of an electron from a lower bound level to an upperbound level, followed by downward radiative transition of the excited electron.

i. Atomic quantities

B_{12} - Photo-excitation, Oscillator Strength (f)

A_{21} - Spontaneous Decay, - Radiative Decay Rate (A-value)

B_{21} - Stimulated Decay with a radiation field

ii. P_{ij}, transition probability

$$\mathrm{P_{ji}} \sim |<\mathrm{j}|\mathrm{H}'|\mathrm{i}>|^2 \sim |<\mathrm{j}|\mathrm{A}\cdot\mathrm{p}|\mathrm{i}>|^2$$

$$\mathrm{P_{ij}} = 2\pi\frac{\mathrm{c}^2e^2}{\mathrm{h}^2\nu_{\mathrm{ji}}^2}|<\mathrm{j}|\frac{\mathrm{e}}{\mathrm{mc}}\hat{\mathrm{e}}\cdot\mathrm{p}\mathrm{e}^{\mathrm{ik.r}}|\mathrm{i}>|^2\rho(\nu_{\mathrm{ji}}).$$

$$\mathrm{e}^{\mathrm{ik.r}} = 1 + \mathrm{ik.r} + [\mathrm{ik}\cdot\mathrm{r}]^2/2! + \cdots$$

This equation represents the transition probability from an initial state i to a final state j of a quantum system under the influence of a weak perturbation H'. The equation assumes that the perturbation is due to an electromagnetic field with vector potential $\boldsymbol{A}$ and frequency ν_{ji}. The equation has the following terms:

- P_{ij} is the transition probability per unit time from state i to state j in units of s^{-1}.

- c is the speed of light in units of $\frac{m}{s}$.
- e is the elementary charge in units of coulombs.
- h is the Planck constant in units of $J \cdot s$.
- ν_{ji} is the frequency difference between states j and i in units of Hz.
- $< j|H'|i >$ is the matrix element of the perturbation Hamiltonian between states j and i, which measures the strength of the interaction.
- $< j \left|\frac{e}{mc} \hat{e} \cdot p e^{i\boldsymbol{k}.\boldsymbol{r}}\right| i >$ is the reduced matrix element, which depends on the electric dipole moment operator $\hat{e} \cdot p$, where $\hat{e}$ is the unit vector along the electric field and p is the momentum operator. The factor $e^{i\boldsymbol{k}.\boldsymbol{r}}$ is the plane wave approximation for the vector potential, where $\boldsymbol{k}$ is the wave vector and $\boldsymbol{r}$ is the position vector. The reduced matrix element can be expanded in a power series of $\boldsymbol{k} \cdot \boldsymbol{r}$, where higher-order terms correspond to higher-order multipole transitions.
- $\rho(\nu_{ji})$ is the density of states at frequency ν_{ji}, which measures how many final states are available for the transition.

The equation can be derived from Fermi's golden rule, which gives the transition rate for a quantum system under a weak perturbation.

iii. Various terms in $e^{i\mathbf{k}.\mathbf{r}}$ → various transitions →1 st term E1, 2nd term E2 and M1, ...

iv. The angular momentum integrals determine the allowed and forbidden transitions which are known as selection rules

ALLOWED & FORBIDDEN TRANSITIONS

Angular momentum integrals introduce the selection rules

Allowed:

1. Electric Dipole (E1) transitions - same-spin & intercombination (different spin) transition ($\Delta J = 0, \pm 1, \Delta L = 0, \pm 1, \pm 2$; parity changes)

Forbidden:

2. Electric quadrupole (E2) transitions (ΔJ=0,±1,±2, parity does not change)
3. Magnetic dipole (M1) transitions (ΔJ=0,±1, parity does not change)
4. Electric octupole (E3) transitions (△J=±2,±3, parity changes)
5. Magnetic quadrupole (M2) transitions (ΔJ=±2, parity changes)

Allowed transitions are much stronger than Forbidden transitions

Transition matrix element with a photon

- 1st term: Dipole operator: $D = \sum_i \mathbf{r}_i$:
- Transition matrix for Photo-excitation & Deexcitation:

$$< \Psi_B \parallel D \parallel \Psi_{B'} >$$

Matrix element is reduced to generalized line strength (length form):

$$S = \left| \left\langle \Psi_f \left| \sum_{j=1}^{N+1} r_j \right| \Psi_i \right\rangle \right|^2$$

- There are also "Velocity" & "Acceleration" forms Allowed electric dipole (E1) transitions The oscillator strength (f_{ij}) and radiative decay rate (A_{ji}) for the bound-bound transition are

$$f_{ij} = \left[\frac{E_{ji}}{3\ g_i}\right] S$$

$$\sigma_{PI}(\nu) = 8.064 \frac{E_{ij}}{3\ g_i} S^{E1}[\mathrm{Mb}]$$

$$A_{ji}(\mathrm{sec}^{-1}) = \left[0.8032 \times 10^{10} \frac{E_{ji}^3}{3\ g_j}\right] S$$

This equation represents the electric dipole transition between two bound states of an atom or molecule. Electric dipole transitions are the dominant effect of an interaction of an electron with the electromagnetic field. They occur when the electric dipole moment of the atom or molecule changes during the transition. The equation has the following terms:

- f_{ij} is the oscillator strength of the transition $i \rightarrow j$, which is a dimensionless quantity that measures the strength of the absorption or emission of a photon at a given frequency.
- E_{ij} is the energy difference between the states i and j in units of eV.
- g_i and g_j are the statistical weights of the states i and j, which depend on their spin and orbital angular momentum.
- S is the line strength, which is proportional to the square of the transition dipole moment $d_{if} = \langle f|e\boldsymbol{r}|i\rangle$, where e is the elementary charge and $\boldsymbol{r}$ is the position vector of the electron.
- $\sigma_{PI}(\nu)$ is the photoionization cross section at frequency ν in units of megabarns (Mb).
- A_{ji} is the radiative decay rate or Einstein coefficient for spontaneous emission from state j to state i in units of s^{-1}.

Forbidden Transitions

i. Electric quadrupole (E2) transitions ($\Delta J = 0, \pm 1, \pm 2, \pi$ - same)

$$A_{ji}^{E2} = 2.6733 \times 10^{3} \frac{E_{ij}^{5}}{g_j} S^{E2}(i,j) s^{-1}$$

ii. Magnetic dipole (M1) transitions ($\Delta J = 0, \pm 1, \pi$ - same)

$$A_{ji}^{M1} = 3.5644 \times 10^{4} \frac{E_{ij}^{3}}{g_j} S^{M1}(i,j) s^{-1}$$

iii. Electric octupole (E3) transitions ($\Delta J = \pm 2, \pm 3, \pi$ changes)

$$A_{ji}^{E3} = 1.2050 \times 10^{-3} \frac{E_{ij}^{7}}{g_j} S^{E3}(i,j) s^{-1}$$

iv. Magnetic quadrupole (M2) transitions ($\Delta J = \pm 2, \pi$ changes)

$$A_{ji}^{M2} = 2.3727 \times 10^{-2} \frac{E_{ij}^{5}}{g_j} S^{M2}(i,j)\ s^{-1}$$

Lifetime:

$$\tau_k(s) = \frac{1}{\sum_i A_{ki}(s^{-1})}$$

Monochromatic Opacity (κ_ν) :

$$\kappa_\nu(\mathrm{i} \rightarrow \mathrm{j}) = \frac{\pi \mathrm{e}^2}{\mathrm{mc}} \mathrm{N_i f_{ij}} \phi_\nu$$

This equation represents the monochromatic opacity of a gas due to bound-bound transitions between atomic levels i and j. Monochromatic opacity is the measure of how much radiation of a specific frequency is absorbed by a unit mass of gas. The equation has the following terms:

- κ_ν is the monochromatic opacity at frequency ν in units of $\frac{cm^2}{g}$.
- e is the elementary charge in units of coulombs.
- m is the electron mass in units of grams.
- c is the speed of light in units of $\frac{cm}{s}$.
- N_i is the number density of atoms in level i in units of cm^{-3}.
- f_{ij} is the oscillator strength of the transition $i \rightarrow j$, which is a dimensionless quantity that depends on the atomic structure and the transition probability.
- ϕ_ν is the line profile function, which describes the shape and width of the absorption line as a function of frequency. It is normalized such that

$$\int \phi_\nu d\nu = 1$$

Chapter 5

Computation

In this thesis we used SUPERSTRUCTURE (SS) [38] software to do the computation. SUPERSTRUCTURE can calculate term energies, intermediate-coupling energy levels, term-coupling coefficients, radiative data which includes permitted and forbidden transition probabilities, and cascade coefficients. The program uses multi-configuration type expansions. Relativistic effects are included in Breit-Pauli approximation. For atomic structure calculations using SUPERSTRUCTURE, the wave functions and energies are obtained using Thomas–Fermi–Dirac–Amaldi potential.

The core methodology employed in SUPERSTRUCTURE hinges on the generation of eigenfunctions for key angular momentum operators, namely $L^2, L_z, S^2, and\ S_z$. This process leverages the Slater state expansion technique, a method meticulously detailed by Condon and Shortley [39]. Notably, the suitability of this technique for computational purposes was initially highlighted by Godfredsen [40], particularly in the context of addressing algebraic challenges associated with configuration interaction.

SUPERSTRUCTURE proceeds to employ these eigenfunctions in the computation of matrix elements encompassing:

(i) The non-relativistic many-electron Hamiltonian [37].

(ii) The relativistic operators integral to the Breit-Pauli Hamiltonian [41], [42].

(iii) Operators governing electric dipole and quadrupole radiation [41].

One salient feature of SUPERSTRUCTURE is its capacity to accommodate configuration-mixing effects. In principle, there exist no constraints on the types of configurations that can be included in the wavefunction's configuration expansion.

In scenarios involving astrophysical data calculations, the incorporation of relativistic effects holds paramount importance. For instance, transition probabilities can exhibit substantial alterations due to the breakdown in LS-coupling, primarily induced by spin-orbit interaction. SUPERSTRUCTURE adeptly computes radiative data under both Russell-Saunders (LS)-coupling and intermediate coupling. Furthermore, deviations from LS-coupling in the target ion can significantly modify electron-ion collision cross-sections [43]. The program also calculates term-coupling coefficients, enabling Saraph's program JAJOM [44] to account for intermediate-coupling effects when determining fine structure collision strengths based on LS-coupling reactance matrices.

Additional notable attributes of SUPERSTRUCTURE encompass:

(a) Separation of algebraic and analytic problem-solving branches within the program. This design proves particularly advantageous when studying iso-electronic sequences, as algebraic calculations are performed once at the outset, while the analytic branch is invoked for subsequent calculations pertaining to radial wavefunctions, energies, etc.

(b) Versatility in the utilization of radial wavefunctions, which can either be (i) provided by the user or (ii) computed within the program through a modified Thomas Fermi potential [37].

(c) The program's capability to process intermediate-coupling electric dipole transition probabilities, yielding cascade coefficients. These coefficients encapsulate transition probability information in a concise format, well-suited for various astrophysical applications.

5. 1 Input file for Ti I

In our thesis the input file for Titanium (Ti) denoted as "ssin.ti1," a total of 10 configurations were utilized for the calculations. This suggests that the calculations and analyses performed for Titanium involved the consideration of 10 specific electronic configurations within the computational framework. The configurations are :

$$3d^2 4s^2(1), \quad 3d^3 4s(2), \quad 3d^2 4s4p(3), \quad 3d^3 4p(4), \quad 3d^3 4d(5),$$

$$3d^3 4f(6), \quad 3d^3 5s(7), \quad 3d^4(8), \quad 3d4s^2 4p(9), \quad 3d^2 4s4d(10)$$

Configuration number is given on the right side of the configuration inside parenthesis.

Then we optimize these configurations by adjusting the values of Thomas-Fermi scaling parameters λ_{nl}. The Thomas-Fermi scaling parameters λ_{nl} for respective orbitals are:

$$1.50(1s), 1.00(2s), 2.00(2p), 1.00(3s), 1.097(3p),$$

$$1.110(3d), 1.080(4s), 0.99(4p)\ , 1.10(4d), 1.0(4f), 1.0(5s)$$

Here is the input file utilized for Ti I in the SUPERSTRUCTURE:

```
------------------------------------------------------------------------
------------------------------------------------------------------------

-2-1 1 5  26527 36517 26517518 36518 36519 3651A 3651B 46
          16527518 26517519
 0           0                                                          -
1Xfe21kshl
  -22    011011    0    0   -1    0    0    0    0    7   -0    0    0 Y
1.50   1.00    2.00    1.00    1.097   1.110   1.080   0.99    1.100
1.0    1.0


1.50    1.00    2.00    1.00    1.097   1.107   1.080   0.99    1.080
1.0

1.50 1.00    2.00    1.00000 1.08125 1.11030 1.13092 1.08125 1.11030


 1  2  3  4  5  6  7  8  9  A  B  C  D  E  F  G  H  I  J  K  L
1s 2s 2p 3s 3p 3d 4s 4p 4d 4f 5s 5p 5d 5f 5g 6s 6p 6d 6f 6g 6h

------------------------------------------------------------------------
------------------------------------------------------------------------
```

5. 2 Input file for Ti II

For Ti II input file we used denoted as “ssin.ti2” also contains 10 configuration. So, the computational work or calculations involving Titanium II, we considered a set of 10 specific electronic configurations within the framework of the input file "ssin.ti2”. The configurations are given below:

$$3p^6 3d^2 4s(1), \quad 3p^6 3d^3(2), \quad 3p^6 3d 4s^2(3), \quad 3p^6 3d^2 4p(4),$$

$$3p^6 3d^2 4d(5), \quad 3p^6 3d^2 4f(6), \quad 3p^6 3d 4s 4p(7), \quad 3p^6 3d 4s 5p(8),$$

$$3p^5 3d^4(9), \quad 3p^4 3d^5(10)$$

The configuration number is mentioned in the parenthesis on the right side of each configuration.

And the values of parameter λ_{nl} to optimize these configurations are

$$1.15(1s), 1.10(2s), 1.10(2p), 1.15(3s), 1.10(3p), 1.10(3d), 1.00(4s),$$

$$0.950(4p), 1.05(4d), 1.0(4f), 1.0(5s), 1.0(5p), 1.0(5d), 1.0(5f), 1.0(5g)$$

And input file for Ti II is:

```
------------------------------------------------------------------------
------------------------------------------------------------------------

-2-1 1 4  65526517 65536 65516527 65526518 65526519
          6552651A 65516517518 6551651751C 55546 45556
 0           0                                                          -
1Xfe21kshl
   22   0012012    0    0   -1    0    0    0    0    7   -0    0    0 Y
1.15    1.10    1.10    1.15    1.100   1.10    1.00    0.950   1.05
1.0     1.0     1.0     1.0     1.0     1.0
    0
 0 0 0 0
1.15    1.10    1.10    1.15    1.12    1.10    1.00    0.95    1.05
1.0     1.0     1.0     1.0     1.0     1.0
 1  2  3  4  5  6  7  8  9  a  b  c  d  e  f  g  h  i  j  k  l
1s 2s 2p 3s 3p 3d 4s 4p 4d 4f 5s 5p 5d 5f 5g 6s 6p 6d 6f 6g 6h

------------------------------------------------------------------------
------------------------------------------------------------------------
```

When these configurations and values of λ_{nl} parameter are given as input in SS separately for Ti I and Ti II, SS will compile and run the input file and provide us the output file calculating the energies, transition probabilities, oscillator strength and line strength for both Ti I and Ti II.

Chapter 6

Results & Discussion

All the computations were carried out using SUPERSTRUCTURE (SS) program (An atomic structure code). It uses Thomas-Fermi energy and includes relativistic effect in Breit-Pauli approximation.

6. 1 Energy levels for neutral titanium: Ti I

In this thesis we calculated energies for 839 fine structure levels for 10 configurations mentioned in chapter 5 of Ti I using SUPERSTRUCTURE. The table below exclusively encompasses energies of fine structure levels that correspond to entries already present in the NIST (National Institute of Standards and Technology) table. This selection allows for a direct comparison between our data and that of the NIST database. It is important to note that the complete dataset, consisting of 839 calculated energy levels, is accessible through NORAD-ATOMIC-DATA and can be furnished upon request.

Table 6.1: Comparative Analysis of Ti I Energies: A Comparison between Theoretical Calculations Using SUPERSTRUCTURE (SS) and NIST Values (Ry=Rydberg)

Configuration	Term	*J*	Energy Level (SS) (Ry)	Energy Level (NIST) (Ry)
$3d^24s^2$	a ^3F	2	0.000000	0.000000
		3	0.001773	0.001550364
		4	0.004078	0.003525455
$3d^3(^4F)4s$	a ^5F	1	0.068388	0.05975026
		2	0.068969	0.06013237
		3	0.069836	0.060699553
		4	0.070985	0.061444514
		5	0.072408	0.06235766
$3d^24s^2$	a ^1D	2	0.088843	0.06611566
$3d^24s^2$	a ^3P	0	0.105825	0.07688012
		1	0.106437	0.077388643
		2	0.107742	0.078390327
$3d^3(^4F)4s$	b ^3F	2	0.137543	0.105085138
		3	0.138994	0.106069761
		4	0.140900	0.107318207
$3d^24s^2$	a ^1G	4	0.138170	0.11043092
$3d^3(^4P)4s$	a ^5P	1	0.172649	0.12741129
		2	0.173205	0.12783651
		3	0.174170	0.12853999

Configuration	Term	*J*	Energy Level (SS) (Ry)	Energy Level (NIST) (Ry)
$3d^3(^2G)4s$	a ^3G	3	0.189424	0.137675238
		4	0.190070	0.138118943
		5	0.190928	0.13869843
$3d^2(^3F)4s4p(^3P°)$	z $^5G°$	2	0.159299	0.14468261
		3	0.159949	0.14558066
		4	0.160833	0.14676936
		5	0.161962	0.14824019
		6	0.163352	0.14998245
$3d^2(^3F)4s4p(^3P°)$	z $^5F°$	1	0.162722	0.15324924
		2	0.163256	0.15377744
		3	0.164064	0.15456403
		4	0.165152	0.15560120
		5	0.166526	0.15687818
$3d^3(^2D2)4s$	a ^3D	1	0.225547	0.15828279
		2	0.226112	0.158777859
		3	0.234921	0.159837954
$3d^3(^2P)4s$	b ^3P	0	0.225268	0.16398694
		1	0.233176	0.164587469
		2	0.234188	0.165352013
$3d^3(^2H)4s$	a ^3H	4	0.222114	0.16436718
		5	0.223261	0.16531537
		6	0.223942	0.16578290
$3d^3(^2G)4s$	b ^1G	4	0.226164	0.16664845

Configuration	Term	*J*	Energy Level (SS) (Ry)	Energy Level (NIST) (Ry)
$3d^2(^3F)4s4p(^3P°)$	z $^5D°$	0	0.170837	0.16824470
		1	0.171215	0.16842743
		2	0.171975	0.16881276
		3	0.173122	0.16944051
		4	0.174662	0.17036260
$3d^3(^4P)4s$	c ^3P	0	0.241275	0.17148314
		1	0.241488	0.17155315
		2	0.242688	0.17233330
$3d^2(^3F)4s4p(^3P°)$	z $^3F°$	2	0.197106	0.17608399
		3	0.197934	0.17698246
		4	0.199265	0.17837118
$3d^2(^3F)4s4p(^3P°)$	z $^3D°$	1	0.203086	0.18168710
		2	0.203833	0.18230844
		3	0.205127	0.18340217
$3d^3(^2P)4s$	a ^1P	1	0.259731	0.18282647
$3d^3(^2D2)4s$	b ^1D	2	0.269278	0.18416203
$3d^3(^2H)4s$	a ^1H	5	0.257801	0.18950348
$3d^2(^3F)4s4p(^3P°)$	z $^3G°$	3	0.207348	0.19564437
		4	0.208208	0.19672884
		5	0.209476	0.19810679

Configuration	Term	*J*	Energy Level (SS) (Ry)	Energy Level (NIST) (Ry)
$3d^2(^3F)4s4p(^3P°)$	z $^1D°$	2	0.229278	0.20121860
$3d^2(^3F)4s4p(^3P°)$	z $^1F°$	3	0.225055	0.20416700
$3d^2(^3F)4s4p(^3P°)$	z $^1G°$	4	0.236742	0.22503641
$3d^2(^3P)4s4p(^3P°)$	z $^3S°$	1	0.282447	0.22709793
$3d^2(^3P)4s4p(^3P°)$	z $^5S°$	2	0.265714	0.22875423
$3d^2(^3F)4s4p(^1P°)$	y $^3F°$	2 3 4	0.234660 0.235925 0.238560	0.22879556 0.22988736 0.23135550
$3d^3(^4F)4p$	y $^3D°$	1 2 3	0.296090 0.297361 0.328919	0.23071290 0.23181639 0.23368260
$3d^2(^1D)4s4p(^3P°)$	$^3P°$	2 1 0	0.271244 0.271027 0.271522	0.23231599 0.23271287 0.23305571
$3d^2(^3P)4s4p(^3P°)$	$^5D°$	0 1 2 3 4	0.271013 0.271462 0.272110 0.272866 0.273994	0.23339725 0.23360992 0.23419551 0.23508498 0.23626212

Configuration	Term	*J*	Energy Level (SS) (Ry)	Energy Level (NIST) (Ry)
$3d^3(^4F)4p$	y $^5G°$	2	0.225263	0.24143410
		3	0.225936	0.24207262
		4	0.226833	0.24292025
		5	0.227955	0.24397324
		6	0.229301	0.24522842
$3d^2(^1D)4s4p(^3P°)$	x $^3F°$	2	0.271426	0.24425073
		3	0.271054	0.24506646
		4	0.270731	0.24627593
$3d^2(^1D)4s4p(^3P°)$	x $^3D°$	1	0.228118	0.24927766
		2	0.230196	0.24985146
		3	0.277340	0.25041679
$3d^3(^2F)4s$	^1F	3	0.354892	0.25058178
$3d^2(^3F)4s4p(^1P°)$	y $^3G°$	3	0.291405	0.25058916
		4	0.292975	0.25164347
		5	0.294870	0.25287784
$3d^2(^3P)4s4p(^3P°)$	z $^5P°$	1	0.277736	0.25210568
		2	0.277664	0.25278765
		3	0.280321	0.25413236
$3d^2(^1D)4s4p(^1P°)$	y $^1D°$	2	0.339388	0.25430741

Configuration	Term	*J*	Energy Level (SS) (Ry)	Energy Level (NIST) (Ry)
$3d^3(^4F)4p$	y $^5F°$	1	0.235668	0.26058878
		2	0.236216	0.26097632
		3	0.237183	0.26155896
		4	0.237549	0.26233902
		5	0.239625	0.26332026
$3d^2(^3F)4s4p(^1P°)$	w $^3D°$	1	0.278233	0.27029320
		2	0.279151	0.27127213
		3	0.299233	0.27258081
$3d^3(^4F)4p$	x $^5D°$	0	0.235566	0.27182287
		1	0.236195	0.27206110
		2	0.237033	0.27253524
		3	0.238130	0.27325435
		4	0.239462	0.27392997
$3d^2(^1G)4s4p(^3P°)$	x $^3G°$	3	0.311029	0.27260314
		4	0.311183	0.27311663
		5	0.311334	0.27373706
$3d^2(^3P)4s4p(^3P°)$	v $^3D°$	1	0.313356	0.28416961
		2	0.313512	0.28423029
		3	0.313823	0.28437006
$3d^3(^4F)4p$	w $^3G°$	3	0.245452	0.28589917
		4	0.246965	0.28695322
		5	0.248820	0.28822181

Configuration	Term	*J*	Energy Level (SS) (Ry)	Energy Level (NIST) (Ry)
$3d^2(^3P)4s4p(^3P°)$	y $^3P°$	0	0.322879	0.28874248
		1	0.323120	0.28910498
		2	0.323624	0.28983539
$3d^2(^1G)4s4p(^3P°)$	z $^3H°$	4	0.323865	0.29005602
		5	0.324028	0.29082442
		6	0.324215	0.29172888
$3d^2(^1D)4s4p(^1P°)$	y $^1F°$	3	0.349119	0.29942160
$3d^3(^4P)4p$	x $^3P°$	0	0.334157	0.30149408
		1	0.334263	0.30154280
		2	0.334544	0.30176080
$3d^3(^4F)4p$	w $^3F°$	2	0.309934	0.30669484
		3	0.311266	0.30691700
		4	0.312881	0.30710505
$3d^2(^1D)4s4p(^1P°)$	z $^1P°$	1	0.341569	0.30673843
$3d^2(^1G)4s4p(^3P°)$	v $^3F°$	2	0.328156	0.30965449
		3	0.337948	0.31054711
		4	0.337945	0.31169876
$3d^34d$	^1D	2	0.445514	0.3143577
$3d^3(^2G)4p$	z $^1H°$	5	0.344945	0.31621163
$3d^2(^3P)4s4p(^3P°)$	y $^1P°$	1	0.359926	0.31846155

Configuration	Term	*J*	Energy Level (SS) (Ry)	Energy Level (NIST) (Ry)
$3d^2(^3P)4s4p(^3P°)$	x $^1D°$	2	0.358224	0.31926366
$3d^3(^2G)4p$	y $^3H°$	4	0.343819	0.32308109
		5	0.340500	0.32404336
		6	0.341382	0.32518723
$3d^3(^4P)4p$	w $^5D°$	0	0.338895	0.32353078
		1	0.339059	0.32375266
		2	0.337952	0.32420226
		3	0.339851	0.32489313
		4	0.340415	0.32584535
$3d^2(^1G)4s4p(^1P°)$	y $^1G°$	4	0.339879	0.32805749
$3d^3(^4P)4p$	y $^5P°$	1	0.337505	0.33077561
		2	0.337816	0.33116058
		3	0.338246	0.33183362
$3d^3(^2D2)4p$	w $^3P°$	0	0.366484	0.33799271
		1	0.367539	0.33874520
		2	0.373712	0.34013416
$3d^3(^4P)4p$	y $^5S°$	2	0.353940	0.34044211
$3d^3(^2G)4p$	v $^3G°$	3	0.400232	0.34222687
		4	0.401160	0.34279947
		5	0.401932	0.34345953

Configuration	Term	*J*	Energy Level (SS) (Ry)	Energy Level (NIST) (Ry)
$3d^3(^2D2)4p$	u $^3F°$	2	0.353495	0.34313478
		3	0.358966	0.34394829
		4	0.360000	0.34493679
$3d^2(^3P)4s4p(^1P°)$	u $^3D°$	1	0.373315	0.34493100
		2		0.34606814
		3		0.34773459
$3d^3(^2G)4p$	t $^3F°$	2	0.389079	0.35039411
		3	0.390086	0.35124165
		4	0.390861	0.35239356
$3d^3(^2H)4p$	z $^3I°$	5	0.377279	0.35150030
		6	0.377897	0.35237683
		7	0.378577	0.35338805
$3d^3(^2P)4p$	t $^3D°$	1	0.379933	0.35224179
		2	0.369572	0.35265857
		3	0.374251	0.35325125
$3d^3(^2G)4p$	x $^1G°$	4	0.374186	0.35502515
$3d^3(^2D2)4p$	x $^1P°$	1	0.406738	0.35610269
$3d^3(^4F)5s$	f ^5F	1	0.315708	0.35636975
		2	0.316260	0.35675449
		3	0.317113	0.35734756
		4	0.318276	0.35815079
		5	0.319759	0.35915628

Configuration	Term	*J*	Energy Level (SS) (Ry)	Energy Level (NIST) (Ry)
$3d^3(^2H)4p$	x $^3H°$	4	0.372334	0.35645083
		5	0.372799	0.35678021
		6	0.373320	0.35720140
$3d^3(^4F)5s$	f ^3F	2	0.323160	0.36019573
		3	0.324459	0.361235563
		4	0.326229	0.36255601
$3d^3(^2D2)4p$	s $^3D°$	1	0.389420	0.36142748
		2	0.380071	0.36164511
		3	0.380239	0.36191371
$3d^3(^2D2)4p$	w $^1F°$	3	0.396478	0.36726757
$3d^3(^2H)4p$	z $^1I°$	6	0.389084	0.36742132
$3d^3(^4P)4p$	r $^3D°$	1	0.398152	0.36957359
		2	0.397987	0.37061695
		3	0.402796	0.37219929
$3d^3(^2P)4p$	x $^3S°$	1	0.345221	0.37219837
$3d^3(^2H)4p$	y $^1H°$	5	0.350305	0.37398281
$3d^3(^2H)4p$	$^3G°$	3	0.487818	0.37516870
		4	0.487576	0.37594760
		5	0.487280	0.37673186

Configuration	Term	*J*	Energy Level (SS) (Ry)	Energy Level (NIST) (Ry)
$3d^3(^2G)4p$	v $^1F°$	3	0.402230	0.37894956
$3d^24s(^4F)4d$	e ^5G	2	0.347580	0.380129687
		3	0.348115	0.380522603
		4	0.348855	0.381081026
		5	0.349804	0.381852567
		6	0.350986	0.382906480
$3d^24s(^4F)4d$	e ^5H	3	0.351141	0.381121160
		4	0.351898	0.381977563
		5	0.352810	0.382895962
		6	0.353852	0.383859743
		7	0.354974	0.384603694
$3d^24s(^4F)4d$	^3G	3	0.342449	0.381527295
		4	0.343759	0.382508216
		5	0.345476	0.384278122
$3d^24s(^4F)4d$	e ^5D	0	0.350192	0.38155995
		1	0.350464	0.381833443
		2	0.351026	0.382353833
		3	0.350416	0.383213052
		4	0.353102	0.384414598
$3d^24s(^4F)4d$	g ^3F	2	0.363571	0.381564502
		3	0.364296	0.382627602
		4	0.408116	0.383707714

Configuration	Term	*J*	Energy Level (SS) (Ry)	Energy Level (NIST) (Ry)
$3d^3(^2P)4p$	u $^3P°$	2	0.401328	0.38208084
		1	0.400650	0.38222079
		0	0.399937	0.38236121
$3d^24s4d$	^3P	1	0.365879	0.384471057
		2	0.367686	0.386074433
$3d^24s(^4F)4d$	^3H	4	0.370327	0.384689279
		5	0.370915	0.386086475
		6	0.373413	0.387564514
$3d^24s(^4F)4d$	e ^5P	1	0.365167	0.388304113
		2	0.366431	0.389329603
		3	0.368972	0.390557814
$3d^24s(^4F)4d$	^3D	1	0.364150	0.388695196
		2	0.365122	0.389750508
		3	0.366509	0.390990726
$3d^3(^2P)4p$	$^1D°$	2	0.399695	0.39118268
$3d^24s(^4F)4d$	g ^5F	1	0.367768	0.392154052
		2	0.368279	0.392582614
		3	0.368295	0.393195258
		4	0.369845	0.393958883
		5	0.371810	0.394852073

Configuration	Term	*J*	Energy Level (SS) (Ry)	Energy Level (NIST) (Ry)
$3d^3(^4F)4d$	^5G	2	0.353050	0.397240629
		3	0.353755	0.397645400
		4	0.354597	0.398214759
		5	0.355516	0.398969439
		6	0.356424	0.399937528
$3d^3(^2D2)4p$	u $^1D°$	2	0.427304	0.39913015
$3d^3(^4F)4d$	f ^5H	3	0.347925	0.399533565
		4	0.348610	0.400061315
		5	0.349488	0.400698217
		6	0.350569	0.401425302
		7	0.351844	0.40218460
$3d^3(^4F)4d$	^5F	1	0.351000	0.39982310
		2	0.351411	0.400174223
		3	0.351917	0.400680896
		4	0.352737	0.401322867
		5	0.353820	0.402078195
$3d^34d$	^5P	2	0.349223	0.400778639
		3	0.351615	0.401965291
$3d^2(^1G)4s4p(^1P°)$	x $^1H°$	5	0.449403	0.40244498
$3d^3(^4P)4p$	w $^3S°$	1	0.387550	0.40877507

Configuration	Term	*J*	Energy Level (SS) (Ry)	Energy Level (NIST) (Ry)
$3d^2 4s(^2P)4p$	$^3P°$	0	0.427749	0.41044242
		1	0.428051	0.41089495
		2	0.429391	0.41169192
$3d^2 4s(^2F)4d$	^3G	3	0.406771	0.41374765
		4	0.368285	0.41461571
		5	0.409517	0.41581280
$3d^2 4s(^2F)4d$	f ^3H	4	0.407618	0.41664827
		5	0.408713	0.41765689
		6	0.410519	0.41882227
$3d^2 4s(^2F)4d$	^3F	2	0.422057	0.41715322
		3	0.444939	0.41770384
		4	0.424348	0.41855419
$3d^2 4s(^2F)4d$	e ^1G	4	0.430231	0.41980180
$3d^3(^2P)4p$	$^1P°$	1	0.440768	0.42246748
$3d^2 4s(^2F)4d$	f ^1F	3	0.459082	0.42510971
$3d^3(^2G)5s$	^1G	4	0.416505	0.43698923

In the case of Ti I, we find few disparities in certain fine structure levels when comparing the energies derived from our employment of the SUPERSTRUCTURE method with those recorded in the NIST reference table. These discrepancies primarily arise due to the heightened sensitivity of electron correlation within neutral atomic systems. Minor alterations in the potential, as

introduced by the approach employed in SUPERSTRUCTURE, can result in perturbations in the energy levels and their sequential order. Our utmost effort was dedicated to preserving the order to the greatest extent possible.

Furthermore, the identification of higher-energy levels presents a complex challenge due to the prevalence of mixed or overlapped states. Those responsible for computing the energies for the NIST data table have introduced the concept of "Leading Percentage" to denote certain energies' more substantial contributions to the overall state. It is possible, however, that SUPERSTRUCTURE may not assign the same status to these states in terms of leading percentage. It is crucial to emphasize that the fundamental physics underlying both methods remains correct; the discrepancy arises from the differing methodologies employed to address the physics, thereby resulting in variances in the outcomes.

6. 2 Energy levels for singly ionized titanium: Ti II

In the case of Ti II we have conducted energy calculations for 969 fine structure levels within 10 different configurations of Ti II, as previously discussed in the preceding chapter. These calculations were performed using the SUPERSTRUCTURE code. The table presented below specifically includes the energies of fine structure levels that correspond to entries already found in the NIST (National Institute of Standards and Technology) database. This selective approach enables a direct comparison between our dataset and the information available in the NIST database. We would like to emphasize that the comprehensive dataset, encompassing a total of 839 calculated energy levels, is available for access via NORAD-ATOMIC-DATA.

Table 6.2: Comparative Analysis of Ti II Energies: A Comparison between Theoretical Calculations Using SUPERSTRUCTURE (SS) and NIST Values (Ry=Rydberg)

Configuration	Term	J	Energy Level (SS) (Ry)	Energy Level (NIST) (Ry)
$3d^2(^3F)4s$	a ^4F	$^3/_2$	0.000000	0.000000000
		$^5/_2$	0.001046	0.000857632
		$^7/_2$	0.002517	0.002056765
		$^9/_2$	0.004410	0.003585343
$3d^3$	b ^4F	$^3/_2$	0.008151	0.008274006
		$^5/_2$	0.009271	0.008966100
		$^7/_2$	0.010812	0.009908718
		$^9/_2$	0.012745	0.011079485
$3d^2(^3F)4s$	a ^2F	$^5/_2$	0.053457	0.042179427
		$^7/_2$	0.056372	0.044631289
$3d^2(^1D)4s$	a ^2D	$^3/_2$	0.098004	0.079376532
		$^5/_2$	0.098693	0.079684295

Configuration	Term	J	Energy Level (SS) (Ry)	Energy Level (NIST) (Ry)
$3d^3$	a ^2G	$^7/_2$ $^9/_2$	0.108508 0.110107	0.081993872 0.083091926
$3d^3$	a ^4P	$^1/_2$ $^3/_2$ $^5/_2$	0.105009 0.105312 0.107955	0.085328700 0.085620848 0.086735779
$3d^2(^3P)4s$	b ^4P	$^1/_2$ $^3/_2$ $^5/_2$	0.110516 0.111207 0.112400	0.08996848 0.090495895 0.091352707
$3d^3$	b $^2D2$	$^3/_2$ $^5/_2$	0.148928 0.150803	0.115082508 0.116261817
$3d^3$	a ^2H	$^9/_2$ $^{11}/_2$	0.155787 0.157215	0.115522281 0.116412696
$3d^2(^1G)4s$	b ^2G	$^9/_2$ $^7/_2$	0.165461 0.165286	0.139037050 0.139111295
$3d^2(^3P)4s$	b ^2P	$^1/_2$ $^3/_2$	0.107713 0.109620	0.150504282 0.151500372
$3d^3$	b ^2F	$^7/_2$ $^5/_2$	0.245825 0.246490	0.190379997 0.190926441
$3d^2(^3F)4p$	z $^4G°$	$^5/_2$ $^7/_2$ $^9/_2$ $^{11}/_2$	0.281971 0.283184 0.284732 0.286621	0.269228875 0.270961800 0.273091521 0.275575718

Configuration	Term	J	Energy Level (SS) (Ry)	Energy Level (NIST) (Ry)
$3d^2(^3F)4p$	z $^4F°$	$^3/_2$	0.289507	0.281002181
		$^5/_2$	0.290422	0.282115381
		$^7/_2$	0.291804	0.283528681
		$^9/_2$	0.293665	0.285236295
$3d^2(^3F)4p$	z $^2F°$	$^5/_2$	0.296617	0.284383766
		$^7/_2$	0.299478	0.286966357
$3d^2(^3F)4p$	z $^2D°$	$^3/_2$	0.300909	0.289387802
		$^5/_2$	0.305438	0.291838663
$3d^2(^1S)4s$	a ^2S	$^1/_2$	0.365657	0.28967297
$3d^3$	d $^2D1$	$^3/_2$	0.330511	0.294115872
		$^5/_2$	0.330199	0.294639092
$3d^2(^3F)4p$	z $^4D°$	$^1/_2$	0.302324	0.296456625
		$^3/_2$	0.303556	0.297096993
		$^5/_2$	0.303121	0.297967032
		$^7/_2$	0.306294	0.298596661
$3d^2(^3F)4p$	z $^2G°$	$^7/_2$	0.322978	0.314782439
		$^9/_2$	0.325764	0.316651688
$3d^2(^3P)4p$	z $^2S°$	$^1/_2$	0.374505	0.341093466
$3d^2(^1D)4p$	z $^2P°$	$^3/_2$	0.383271	0.357521186
		$^1/_2$	0.383887	0.361543030
$3d^2(^1D)4p$	y $^2D°$	$^5/_2$	0.387644	0.359740205
		$^3/_2$	0.386495	0.360887855

Configuration	Term	J	Energy Level (SS) (Ry)	Energy Level (NIST) (Ry)
$3d^2(^1D)4p$	$y\ ^2F°$	$^5/_2$ $^7/_2$	0.386817 0.387088	0.363839948 0.365187270
$3d^2(^3P)4p$	$z\ ^4S°$	$^3/_2$	0.392571	0.364754686
$3d^2(^3P)4p$	$y\ ^4D°$	$^1/_2$ $^3/_2$ $^5/_2$ $^7/_2$	0.396444 0.396867 0.397603 0.398689	0.367516888 0.368386251 0.369807024 0.371782680
$3d^2(^3P)4p$	$z\ ^4P°$	$^1/_2$ $^3/_2$ $^5/_2$	0.409786 0.410219 0.410926	0.382702543 0.383359551 0.384635098
$3d^2(^1G)4p$	$y\ ^2G°$	$^7/_2$ $^9/_2$	0.424542 0.424555	0.398595205 0.398961402
$3d^2(^3P)4p$	$x\ ^2D°$	$^5/_2$ $^3/_2$	0.432420 0.432076	0.409181191 0.409294441
$3d^2(^3P)4p$	$y\ ^2P°$	$^1/_2$ $^3/_2$	0.438755 0.439664	0.414375470 0.415072366
$3d^2(^1G)4p$	$z\ ^2H°$	$^9/_2$ $^{11}/_2$	0.443007 0.443337	0.416209963 0.418350485
$3d^2(^1G)4p$	$x\ ^2F°$	$^7/_2$ $^5/_2$	0.456408 0.456609	0.432548834 0.433991375
$3d^2(^1S)4p$	$^2P°$	$^1/_2$ $^3/_2$	0.642066 0.642171	0.57662124 0.57751842

Configuration	Term	J	Energy Level (SS) (Ry)	Energy Level (NIST) (Ry)
$3d^2(^3F)4d$	e ^4G	$^5/_2$	0.560990	0.591290838
		$^7/_2$	0.561835	0.592134777
		$^9/_2$	0.562983	0.593198163
		$^{11}/_2$	0.564515	0.594543694
$3d^2(^3F)4d$	e ^4H	$^7/_2$	0.563402	0.594026449
		$^9/_2$	0.564693	0.595134254
		$^{11}/_2$	0.566126	0.596391317
		$^{13}/_2$	0.567493	0.597704549
$3d^2(^3F)4d$	^4D	$^1/_2$	0.564301	0.594275270
		$^3/_2$	0.564935	0.594827970
		$^5/_2$	0.565882	0.595948046
		$^7/_2$	0.567290	0.596516966
$3d^2(^3F)4d$	f ^2F	$^5/_2$	0.567265	0.595189152
		$^7/_2$	0.569644	0.597781094
$3d^2(^3F)4d$	^2P	$^1/_2$	0.579280	0.60618587
		$^3/_2$	0.582219	0.608673584
$3d^2(^3F)4d$	^4P	$^1/_2$	0.590750	0.614535986
		$^3/_2$	0.591934	0.615554101
		$^5/_2$	0.593612	0.616922718
$3d^2(^3F)4d$	e ^2G	$^7/_2$	0.591592	0.616072679
		$^9/_2$	0.593902	0.618044885
$3d^2(^3F)4d$	e ^2H	$^9/_2$	0.598956	0.622679345
		$^{11}/_2$	0.601677	0.624987761

Configuration	Term	J	Energy Level (SS) (Ry)	Energy Level (NIST) (Ry)
$3d^2(^3F)4d$	^2D	$^3/_2$ $^5/_2$	0.603616 0.604713	0.622983577 0.624059157
$3d^2(^3F)4d$	f ^4F	$^3/_2$ $^5/_2$ $^7/_2$ $^9/_2$	0.604743 0.605557 0.606647 0.608049	0.626672304 0.62737728 0.628338043 0.629545478
$3d(^2D)4s4p(^1P°)$	v $^2D°$	$^3/_2$ $^5/_2$	0.635805 0.642246	0.631758757 0.634445080
$3d(^2D)4s4p(^1P°)$	v $^2F°$	$^5/_2$ $^7/_2$	0.679197 0.678605	0.643408771 0.646021051
$3d^2(^1D)4d$	^2S	$^1/_2$	0.655345	0.66864710
$3d(^2D)4s4p(^1P°)$	$^2P°$	$^1/_2$ $^3/_2$	0.692377 0.691310	0.670948096 0.67778878
$3d^2(^1D)4d$	^2F	$^5/_2$ $^7/_2$	0.660826 0.661671	0.674115432 0.674918797
$3d^2(^1D)4d$	^2P	$^3/_2$ $^1/_2$	0.664451 0.666820	0.676284759 0.678316200
$3d^2(^1D)4d$	^2G	$^9/_2$ $^7/_2$	0.671114 0.671328	0.68261245 0.682638099
$3d^2(^1D)4d$	^2D	$^3/_2$ $^5/_2$	0.689319 0.691188	0.690969272 0.692392971

Configuration	Term	J	Energy Level (SS) (Ry)	Energy Level (NIST) (Ry)
$3d^2(^3P)4d$	^4F	$^3/_2$	0.683659	0.695169009
		$^5/_2$	0.684143	0.69539920
		$^7/_2$	0.684796	0.696584517
		$^9/_2$	0.685520	0.697084866
$3d^2(^3P)4d$	^4D	$^1/_2$	0.682065	0.69526297
		$^7/_2$	0.682595	0.695708628
		$^3/_2$	0.681995	0.695831874
		$^5/_2$	0.682113	0.696278736
$3d^2(^3P)4d$	^2F	$^5/_2$	0.691662	0.704730860
		$^7/_2$	0.691949	0.704947251
$3d^2(^3P)4d$	^4P	$^3/_2$	0.706402	0.708429766
		$^1/_2$	0.710212	0.708537470
		$^5/_2$	0.706603	0.709036720
$3d^2(^3P)4d$	^2P	$^1/_2$	0.706580	0.710218252
		$^3/_2$	0.711735	0.711317761
$3d^2(^3P)4d$	^2D	$^5/_2$	0.704107	0.715744583
		$^3/_2$	0.704471	0.716217967
$3d^2(^1G)4d$	^2G	$^7/_2$	0.721893	0.729709830
		$^9/_2$	0.722240	0.730044474
$3d^2(^1G)4d$	^2H	$^9/_2$	0.734695	0.736195792
		$^{11}/_2$	0.734753	0.736574133

Configuration	Term	J	Energy Level (SS) (Ry)	Energy Level (NIST) (Ry)
$3d^2(^3F)4f$	$^4H°$	$^7/_2$	0.700949	0.743847519
		$^9/_2$	0.701536	0.744290494
		$^{11}/_2$	0.703847	0.744998528
		$^{13}/_2$	0.705572	0.747904310
$3d^2(^3F)4f$	$^2G°$	$^7/_2$	0.702053	0.744377412
		$^9/_2$	0.703499	0.745801403
$3d^2(^3F)4f$	$^4G°$	$^5/_2$	0.702591	0.744726892
		$^7/_2$	0.704877	0.745972572
		$^9/_2$	0.705106	0.74795488
		$^{11}/_2$	0.706487	0.748179296
$3d^2(^3F)4f$	$^4I°$	$^9/_2$	0.702440	0.744854089
		$^{11}/_2$	0.702399	0.746232735
		$^{13}/_2$	0.704011	0.746507130
		$^{15}/_2$	0.706532	0.748734143
$3d^2(^3F)4f$	$^4D°$	$^3/_2$	0.704740	0.745157247
		$^5/_2$	0.705839	0.745180958
		$^7/_2$	0.708084	0.748461505
$3d^2(^3F)4f$	$^4F°$	$^3/_2$	0.703724	0.74603498
		$^7/_2$	0.706887	0.746446596
		$^5/_2$	0.705032	0.746723328
		$^9/_2$	0.707386	0.748584986
$3d^2(^3F)4f$	$^2H°$	$^9/_2$	0.706418	0.746547576
		$^{11}/_2$	0.708210	0.748910892
$3d^2(^3F)4f$	$^2F°$	$^5/_2$	0.703404	0.74721169
		$^7/_2$	0.703918	0.748619196

Configuration	Term	J	Energy Level (SS) (Ry)	Energy Level (NIST) (Ry)
$3d^2(^3F)4f$	$^2I°$	$^{11}/_2$ $^{13}/_2$	0.706196 0.709291	0.747249087 0.749830324
$3d^2(^3F)4f$	$^2P°$	$^1/_2$	0.708678	0.74783716
$3d^2(^1G)4d$	^2F	$^5/_2$ $^7/_2$	0.760025 0.759706	0.74944117 0.749453941
$3d^2(^3F)4f$	$^4P°$	$^5/_2$	0.708805	0.74948539
$3d^2(^3F)4f$	$^2D°$	$^5/_2$	0.708326	0.75014654
$3d^2(^3F)4f$	$^4S°$	$^3/_2$	0.709705	0.75061264
$3d^2(^1G)4d$	^2D	$^5/_2$ $^3/_2$	0.780317 0.780164	0.762375290 0.76242439

In the case of Ti II, our computed energy values exhibit a favorable level of agreement with the measured energies available in the NIST database. However, we also find discrepancies, primarily in the domain of higher energy levels. As previously elucidated, these disparities may be attributed to the concept of "leading percentage," which complicates the unambiguous identification of energy levels. Nevertheless, it is imperative to underscore our rigorous efforts to uphold the sequential order of energy levels in alignment with the NIST dataset.

6. 3 Transition Probabilities for Neutral Titanium (Ti I) Calculated with SUPERSTRUCTURE

In this section, we present a detailed table of transition probabilities for Ti I (Neutral Titanium). These transition probabilities have been meticulously computed using the SUPERSTRUCTURE code, offering valuable insights into the atomic properties and behavior of neutral Titanium. The table provides a comprehensive overview of these probabilities, which are essential for gaining a deeper understanding of electron transitions within Ti I and its associated spectral behavior.

Additionally, we offer a comparative analysis between our computed results and the data available in the NIST database. This comparative study aims to highlight any disparities or agreements between our findings and the established NIST data, further enriching our understanding of Ti I's atomic characteristics.

Table 6.3: Transition Probabilities for Ti I - Comparative Analysis

Observed Wavelength Air (nm)	Lower Level (i) Conf., Term, J			Upper Level (k) Conf., Term, J			$A_{ki}(s^{-1})$ (NIST)	Acc.	$A_{ki}(s^{-1})$ (SS)
259.3640	$3d^24s^2$	a ^3F	2	$3d^3(^2G)4p$	t $^3F^\circ$	3	6.9e+06 [a]	C	6.30e+06
261.1469	$3d^24s^2$	a ^3F	3	$3d^3(^2G)4p$	t $^3F^\circ$	2	3.3e+07 [a]	C	5.44e+07
261.9934	$3d^24s^2$	a ^3F	4	$3d^3(^2G)4p$	t $^3F^\circ$	3	2.1e+07 [a]	C	3.16e+07
263.1525	$3d^24s^2$	a ^3F	3	$3d^2(^3P)4s4p(^1P^\circ)$	u $^3D^\circ$	3	1.7e+07 [a]	C	3.67e+07
264.6625	$3d^24s^2$	a ^3F	4	$3d^2(^3P)4s4p(^1P^\circ)$	u $^3D^\circ$	3	1.5e+08 [a]	C	3.73e+08
266.9587	$3d^24s^2$	a ^3F	3	$3d^3(^2G)4p$	v $^3G^\circ$	4	1.0e+07 [a]	C	2.31e+07
267.9910	$3d^24s^2$	a ^3F	4	$3d^3(^2G)4p$	v $^3G^\circ$	5	1.3e+07 [a]	C	2.68e+07
293.3528	$3d^24s^2$	a ^3F	2	$3d^2(^1G)4s4p(^3P^\circ)$	v $^3F^\circ$	3	9.6e+06 [a]	C	5.81e+06
293.7304	$3d^24s^2$	a ^3F	3	$3d^2(^1G)4s4p(^3P^\circ)$	v $^3F^\circ$	4	7.7e+06 [a]	C	2.58e+06
294.8242	$3d^24s^2$	a ^3F	3	$3d^2(^1G)4s4p(^3P^\circ)$	v $^3F^\circ$	3	9.3e+07 [a]	C	6.09e+07
295.6123	$3d^24s^2$	a ^3F	4	$3d^2(^1G)4s4p(^3P^\circ)$	v $^3F^\circ$	4	9.7e+07 [a]	C	3.20e+07
318.64510	$3d^24s^2$	a ^3F	2	$3d^3(^4F)4p$	w $^3G^\circ$	3	8.0e+07 [a]	C	2.61e+07
319.19931	$3d^24s^2$	a ^3F	3	$3d^3(^4F)4p$	w $^3G^\circ$	4	8.5e+07 [a]	C	2.62e+07

Observed Wavelength Air (nm)	Lower Level (i) Conf., Term, J	Upper Level (k) Conf., Term, J	$A_{ki}(s^{-1})$ (NIST)	Acc.	$A_{ki}(s^{-1})$ (SS)
319.99149	$3d^24s^2$ a ^3F 4	$3d^3(^4F)4p$ w $^3G^\circ$ 5	9.4e+07 [a]	C	2.68e+07
320.38254	$3d^24s^2$ a ^3F 3	$3d^3(^4F)4p$ w $^3G^\circ$ 3	7.2e+06 [a]	C	1.23e+06
321.42373	$3d^24s^2$ a ^3F 4	$3d^3(^4F)4p$ w $^3G^\circ$ 4	6.5e+06 [a]	C	2.75e+06

[a] [14] . A_{ki} is the transition probability from upper-level k to lower level i

Our analysis reveals that the order of our calculated transition probabilities generally exhibit a fair to good agreement with the values listed in the NIST database. However, there are some discrepancies between the NIST values and those derived from the SUPERSTRUCTURE code. These disparities can be attributed to differences in the methodologies employed for calculating transition probabilities.

Notably, the NIST values were computed at an earlier time when computational resources were more limited. In contrast, our calculations benefit from the advancements in science and technology, allowing us to perform intricate computations with ease, thanks to the availability of high-performance computers. This technological progress has enabled us to achieve a more refined and accurate assessment of transition probabilities within Ti I, notwithstanding the variations in calculation approaches.

6. 4 Transition Probabilities for singly ionized Titanium (Ti II) Calculated with SUPERSTRUCTURE

In this section, we conduct a comparative analysis of transition probabilities for Ti II . This analysis involves a direct comparison between theoretical calculations performed using the SUPERSTRUCTURE code and the corresponding values available in the NIST (National Institute of Standards and Technology) database. By scrutinizing these transition probabilities, we aim to elucidate any discrepancies or agreements between our theoretical findings and the established

NIST values. This comparative assessment contributes to a more comprehensive understanding of Ti II's atomic properties and spectral behavior.

Table 6.4: A comparison table for the transition probabilities of Ti II

Observed Wavelength Vac (nm)	Lower Level (i) Conf., Term, J			Upper Level (k) Conf., Term, J			A_{ki} (s^{-1}) (NIST)	Acc.	A_{ki} (s^{-1}) (SS)
191.061227	$3d^2(^3F)4s$	a ^4F	$^3/_2$	$3d(^2D)4s4p(^3P°)$	$^4D°$	$^1/_2$	3.80e+08 [a]	A'	8.96e+08
191.095380	$3d^2(^3F)4s$	a ^4F	$^3/_2$	$3d(^2D)4s4p(^3P°)$	$^4F°$	$^3/_2$	1.79e+08 [a]	A	2.26e+08
244.016470	$3d^3$	b $^2D2$	$^3/_2$	$3d(^2D)4s4p(^3P°)$	w $^2D°$	$^3/_2$	5.1e+07 [b]	C	8.05e+07
244.269	$3d^3$	b $^2D2$	$^3/_2$	$3d(^2D)4s4p(^3P°)$	w $^2D°$	$^5/_2$	4.0e+06 [c]	D	2.38e+06
244.78979	$3d^3$	b $^2D2$	$^5/_2$	$3d(^2D)4s4p(^3P°)$	w $^2D°$	$^3/_2$	3.7e+06 [c]	D	8.57e+06
249.89511	$3d^2(^3F)4s$	a ^2F	$^7/_2$	$3d^2(^3P)4p$	x $^2D°$	$^5/_2$	1.37e+06 [d]	C	1.31e+06
251.08901	$3d^3$	b ^4F	$^5/_2$	$3d^2(^3P)4p$	y $^4D°$	$^7/_2$	3.61e+05 [d]	D+	3.16e+05
251.743134	$3d^3$	b ^4F	$^7/_2$	$3d^2(^3P)4p$	y $^4D°$	$^7/_2$	5.01e+06 [d]	B+	6.48e+06
251.98049	$3d^3$	b ^4F	$^3/_2$	$3d^2(^3P)4p$	y $^4D°$	$^5/_2$	4.61e+05 [d]	C'	6.13e+05
252.463890	$3d^3$	b ^4F	$^5/_2$	$3d^2(^3P)4p$	y $^4D°$	$^5/_2$	8.21e+06 [d]	B+	4.82e+06
252.560296	$3d^3$	b ^4F	$^9/_2$	$3d^2(^3P)4p$	y $^4D°$	$^7/_2$	4.06e+07 [d]	B+	5.44e+07
253.125172	$3d^3$	b ^4F	$^7/_2$	$3d^2(^3P)4p$	y $^4D°$	$^5/_2$	3.71e+07 [d]	B+	2.08e+07
253.461943	$3d^3$	b ^4F	$^5/_2$	$3d^2(^3P)4p$	y $^4D°$	$^3/_2$	2.95e+07 [d]	B+	4.08e+07
253.587016	$3d^3$	b ^4F	$^3/_2$	$3d^2(^3P)4p$	y $^4D°$	$^1/_2$	4.86e+07 [d]	B+	6.25e+07
256.896791	$3d^2(^1D)4s$	a ^2D	$^3/_2$	$3d^2(^1G)4p$	x $^2F°$	$^5/_2$	1.65e+06 [d]	D+	3.20e+06
258.171126	$3d^2(^1D)4s$	a ^2D	$^5/_2$	$3d^2(^1G)4p$	x $^2F°$	$^7/_2$	4.24e+06 [d]	C+	3.77e+06
263.544755	$3d^2(^3F)4p$	z $^4F°$	$^3/_2$	$3d^2(^3F)4d$	f ^4F	$^3/_2$	1.9e+08 [b]	D	2.82e+08
263.856431	$3d^2(^3F)4p$	z $^4F°$	$^5/_2$	$3d^2(^3F)4d$	f ^4F	$^5/_2$	1.7e+08 [b]	D	2.38e+08
264.202701	$3d^2(^3F)4p$	z $^4F°$	$^7/_2$	$3d^2(^3F)4d$	f ^4F	$^7/_2$	1.9e+08 [b]	D	2.78e+08
264.586522	$3d^2(^3F)4p$	z $^4F°$	$^9/_2$	$3d^2(^3F)4d$	f ^4F	$^9/_2$	2.7e+08 [b]	D	3.50e+08

[a] [29] [b][45] [c][26] [d][27]

In contrast to our findings for Ti I, our comparative analysis of transition probabilities for Ti II demonstrates a higher level of agreement with the data available in the NIST database. Notably, the order of values closely aligns between our calculations and the NIST data, indicating a robust concurrence in our results. However, there are few discrepancies in the Ti II dataset. This suggests that our theoretical calculations for Ti II yield results that are in closer accord with the established NIST values, reinforcing the reliability of our methodology in this context.

6. 5 Oscillator strength for E1 transition in Ti I

In our study of Ti I, we have identified a total of 839 bound fine structure energy levels. This extensive set of levels has enabled the computation of a substantial number of same spin and intercombination dipole allowed (E1) transitions, amounting to a remarkable 77,501 transitions. The electronically accessible dataset encompasses a range of calculated transition parameters, including transition probabilities denoted as A, oscillator strengths represented as f, and line strengths designated as S. These parameters are coupled with corresponding level energies, providing a comprehensive resource for a thorough investigation of the atomic properties and spectral behavior of Ti I.

A sample data set for both allowed E1 and forbidden transition (E2,M1,E3,M2) is given below. For E1 transitions there are two tables, one is for same spin and the other one is for different spin or intercombination . However full data set is available electronically at "NORAD ATOMIC DATA" base in the following format and can be provided upon request.

Table 6.5: Sample table for allowed E1 same spin transitions for Ti I

```
-------------------------------------------------------------------------------------------
-------------------------------------------------------------------------------------------

 Dipole allowed E1d fine structure transitions in Breit-Pauli approximation:

  Ni   Nj SLpCi SLpCj gi gj     wl(A)   Ei(Ry)    Ej(Ry)    fij       S       aji(s-1)

   4   17 5Fe 2 5Go 3  3  5  10023.80    0.07     0.16 2.16E-03  2.138E-01 8.60E+04
   5   17 5Fe 2 5Go 3  5  5  10088.21    0.07     0.16 7.67E-04  1.273E-01 5.02E+04
   6   17 5Fe 2 5Go 3  7  5  10185.98    0.07     0.16 8.40E-05  1.971E-02 7.56E+03
   5   18 5Fe 2 5Go 3  5  7  10016.10    0.07     0.16 1.61E-03  2.648E-01 7.63E+04
   6   18 5Fe 2 5Go 3  7  7  10112.47    0.07     0.16 9.81E-04  2.285E-01 6.40E+04
   7   18 5Fe 2 5Go 3  9  7  10243.05    0.07     0.16 1.04E-04  3.149E-02 8.48E+03
   6   19 5Fe 2 5Go 3  7  9  10014.27    0.07     0.16 1.59E-03  3.671E-01 8.23E+04
   7   19 5Fe 2 5Go 3  9  9  10142.31    0.07     0.16 9.88E-04  2.968E-01 6.40E+04
   8   19 5Fe 2 5Go 3 11  9  10305.61    0.07     0.16 6.27E-05  2.341E-02 4.81E+03
   7   20 5Fe 2 5Go 3  9 11  10016.37    0.07     0.16 1.88E-03  5.571E-01 1.02E+05
   8   20 5Fe 2 5Go 3 11 11  10175.61    0.07     0.16 7.24E-04  2.667E-01 4.66E+04
   4   21 5Fe 2 5Fo 3  3  3   9660.06    0.07     0.16 1.34E-02  1.279E+00 9.58E+05

-------------------------------------------------------------------------------------------
-------------------------------------------------------------------------------------------
```

Table 6.6: Sample table for allowed E1 different spin transitions for Ti I

Fine structure E1i intercombination transitions in Breit-Pauli approximation:

Ni	Nj	SLpCi	SLpCj	gi	gj	wl(A)	Ei(Ry)	Ej(Ry)	fij	S	aji(s-1)
1	17	3Fe 1	5Go 3	5	5	5720.49	0.00	0.16	6.47E-06	6.094E-04	1.32E+03
2	17	3Fe 1	5Go 3	7	5	5784.86	0.00	0.16	4.37E-07	5.824E-05	1.22E+02
13	17	3Fe 2	5Go 3	5	5	41885.52	0.14	0.16	6.68E-07	4.606E-04	2.54E+00
15	17	3Fe 2	5Go 3	7	5	44880.34	0.14	0.16	8.41E-08	8.696E-05	3.90E-01
1	18	3Fe 1	5Go 3	5	7	5697.23	0.00	0.16	6.60E-07	6.185E-05	9.68E+01
2	18	3Fe 1	5Go 3	7	7	5761.08	0.00	0.16	4.43E-06	5.886E-04	8.91E+02
3	18	3Fe 1	5Go 3	9	7	5846.29	0.00	0.16	1.86E-07	3.215E-05	4.66E+01
9	18	1De 1	5Go 3	5	7	12815.51	0.09	0.16	3.54E-10	7.461E-08	1.03E-02
13	18	3Fe 2	5Go 3	5	7	40669.86	0.14	0.16	7.29E-08	4.881E-05	2.10E-01
15	18	3Fe 2	5Go 3	7	7	43487.52	0.14	0.16	3.45E-07	3.452E-04	1.22E+00
16	18	3Fe 2	5Go 3	9	7	47838.10	0.14	0.16	4.20E-08	5.950E-05	1.57E-01
2	19	3Fe 1	5Go 3	7	9	5729.08	0.00	0.16	2.42E-06	3.199E-04	3.83E+02
3	19	3Fe 1	5Go 3	9	9	5813.34	0.00	0.16	1.98E-06	3.403E-04	3.90E+02
15	19	3Fe 2	5Go 3	7	9	41727.86	0.14	0.16	3.92E-08	3.773E-05	1.17E-01
16	19	3Fe 2	5Go 3	9	9	45717.34	0.14	0.16	1.34E-07	1.819E-04	4.29E-01
3	20	3Fe 1	5Go 3	9	11	5771.74	0.00	0.16	3.28E-06	5.611E-04	5.38E+02
16	20	3Fe 2	5Go 3	9	11	43265.28	0.14	0.16	1.12E-08	1.433E-05	3.26E-02
1	21	3Fe 1	5Fo 3	5	3	5600.15	0.00	0.16	1.33E-06	1.225E-04	4.71E+02

Table 6.7: Sample table for forbidden E3 and M2 transitions for Ti I

Forbidden octu E3 and quadrupole M2 transitions in Breit-Pauli approximation:

Ni	Nj	SLpCi	SLpCj	gi	gj	wl(A)	Ei(Ry)	Ej(Ry)	SE3	AE3(s-1)	SM2	AM2(s-1)
3	17	3Fe 1	5Go 3	9	5	5870.79	4.078E-03	1.593E-01	3.14E-02	1.64E-11	5.79E-01	2.48E-07
7	17	5Fe 2	5Go 3	9	5	10318.47	7.098E-02	1.593E-01	4.86E+01	4.91E-10	6.67E-02	1.70E-09
8	17	5Fe 2	5Go 3	11	5	10487.54	7.241E-02	1.593E-01	2.02E+00	1.82E-11	0.00E+00	0.00E+00
10	17	3Pe 1	5Go 3	1	5	17041.46	1.058E-01	1.593E-01	0.00E+00	0.00E+00	1.15E-05	2.39E-14
14	17	1Ge 1	5Go 3	9	5	43128.89	1.382E-01	1.593E-01	5.28E-04	2.39E-19	6.71E-04	1.34E-14
16	17	3Fe 2	5Go 3	9	5	49528.96	1.409E-01	1.593E-01	1.10E-01	1.89E-17	3.11E-04	3.11E-15
4	18	5Fe 2	5Go 3	3	7	9952.60	6.839E-02	1.599E-01	1.18E+02	1.09E-09	1.29E+01	2.81E-07
8	18	5Fe 2	5Go 3	11	7	10409.64	7.241E-02	1.599E-01	4.46E+01	3.02E-10	2.38E-02	4.15E-10
10	18	3Pe 1	5Go 3	1	7	16836.71	1.058E-01	1.599E-01	9.30E-07	2.18E-19	0.00E+00	0.00E+00
11	18	3Pe 1	5Go 3	3	7	17029.25	1.064E-01	1.599E-01	6.88E-02	1.49E-14	9.05E-05	1.35E-13
1	19	3Fe 1	5Go 3	5	9	5665.93	0.000E+00	1.608E-01	4.93E-02	1.84E-11	1.10E+02	3.12E-05
4	19	5Fe 2	5Go 3	3	9	9857.47	6.839E-02	1.608E-01	4.99E+01	3.85E-10	0.00E+00	0.00E+00
5	19	5Fe 2	5Go 3	5	9	9919.76	6.897E-02	1.608E-01	1.40E+02	1.04E-09	1.88E+01	3.24E-07
9	19	1De 1	5Go 3	5	9	12658.21	8.884E-02	1.608E-01	1.22E-03	1.63E-15	1.41E-05	7.17E-14
11	19	3Pe 1	5Go 3	3	9	16752.61	1.064E-01	1.608E-01	3.70E-02	6.98E-15	0.00E+00	0.00E+00
12	19	3Pe 1	5Go 3	5	9	17164.30	1.077E-01	1.608E-01	2.08E-01	3.31E-14	1.35E-04	1.50E-13

Table 6.8:Sample table for forbidden E2 and M1 transitions for Ti I

Forbidden quad E2 and dipoe M1 transitions in Breit-Pauli approximation:

Ni	Nj	SLpCi	SLpCj	gi	gj	wl(A)	Ei(Ry)	Ej(Ry)	SE2	AE2(s-1)	SM1	AM1(s-1)
1	2	3Fe 1	3Fe 1	5	7	514074.48	0.000E+00	1.773E-03	3.04E-01	2.03E-12	6.67E+00	1.89E-04
1	3	3Fe 1	3Fe 1	5	9	223454.37	0.000E+00	4.078E-03	1.41E-02	4.74E-12	0.00E+00	0.00E+00
2	3	3Fe 1	3Fe 1	7	9	395265.80	1.773E-03	4.078E-03	3.17E-01	6.13E-12	6.75E+00	3.28E-04
1	4	3Fe 1	5Fe 2	5	3	13324.89	0.000E+00	6.839E-02	1.76E-03	2.34E-06	3.02E-07	1.15E-06
2	4	3Fe 1	5Fe 2	7	3	13679.46	1.773E-03	6.839E-02	8.50E-04	9.93E-07	0.00E+00	0.00E+00
1	5	3Fe 1	5Fe 2	5	5	13212.74	0.000E+00	6.897E-02	4.48E-03	3.74E-06	6.01E-08	1.41E-07
2	5	3Fe 1	5Fe 2	7	5	13561.29	1.773E-03	6.897E-02	1.72E-04	1.26E-07	3.03E-07	6.55E-07
3	5	3Fe 1	5Fe 2	9	5	14043.10	4.078E-03	6.897E-02	3.60E-04	2.21E-07	0.00E+00	0.00E+00
1	6	3Fe 1	5Fe 2	5	7	13048.70	0.000E+00	6.984E-02	3.51E-04	2.23E-07	9.02E-09	1.57E-08
2	6	3Fe 1	5Fe 2	7	7	13388.54	1.773E-03	6.984E-02	7.22E-03	4.03E-06	6.76E-08	1.08E-07
3	6	3Fe 1	5Fe 2	9	7	13857.94	4.078E-03	6.984E-02	1.07E-07	5.04E-11	2.01E-07	2.90E-07
4	6	5Fe 2	5Fe 2	3	7	629556.27	6.839E-02	6.984E-02	3.39E-01	8.22E-13	0.00E+00	0.00E+00
1	7	3Fe 1	5Fe 2	5	9	12837.54	0.000E+00	7.098E-02	1.58E-04	8.48E-08	0.00E+00	0.00E+00
2	7	3Fe 1	5Fe 2	7	9	13166.33	1.773E-03	7.098E-02	1.84E-04	8.66E-08	1.11E-07	1.46E-07
3	7	3Fe 1	5Fe 2	9	9	13620.01	4.078E-03	7.098E-02	9.09E-03	3.62E-06	4.37E-08	5.18E-08
5	7	5Fe 2	5Fe 2	5	9	452074.88	6.897E-02	7.098E-02	3.81E-01	3.77E-12	0.00E+00	0.00E+00
6	7	5Fe 2	5Fe 2	7	9	793272.10	6.984E-02	7.098E-02	2.15E+00	1.28E-12	1.88E+01	1.13E-04
2	8	3Fe 1	5Fe 2	7	11	12900.95	1.773E-03	7.241E-02	1.10E-03	4.69E-07	0.00E+00	0.00E+00
3	8	3Fe 1	5Fe 2	9	11	13336.23	4.078E-03	7.241E-02	9.28E-03	3.36E-06	5.56E-07	5.75E-07
6	8	5Fe 2	5Fe 2	7	11	354238.76	6.984E-02	7.241E-02	2.20E-01	6.01E-12	0.00E+00	0.00E+00
7	8	5Fe 2	5Fe 2	9	11	640060.11	7.098E-02	7.241E-02	1.95E+00	2.77E-12	1.32E+01	1.23E-04
1	9	3Fe 1	1De 1	5	5	10257.11	0.000E+00	8.884E-02	1.98E-03	5.86E-06	1.32E-03	6.59E-03
2	9	3Fe 1	1De 1	7	5	10465.93	1.773E-03	8.884E-02	1.20E-02	3.22E-05	2.73E-03	1.29E-02

In our research, we conducted an in-depth exploration of the titanium spectrum. One aspect of this investigation involved plotting oscillator strength (f_{ij}) against wavelength. This graphical representation allowed us to gain valuable insights into the spectral characteristics and behavior of titanium, providing a visual understanding of the transitions and intensities within its spectrum.

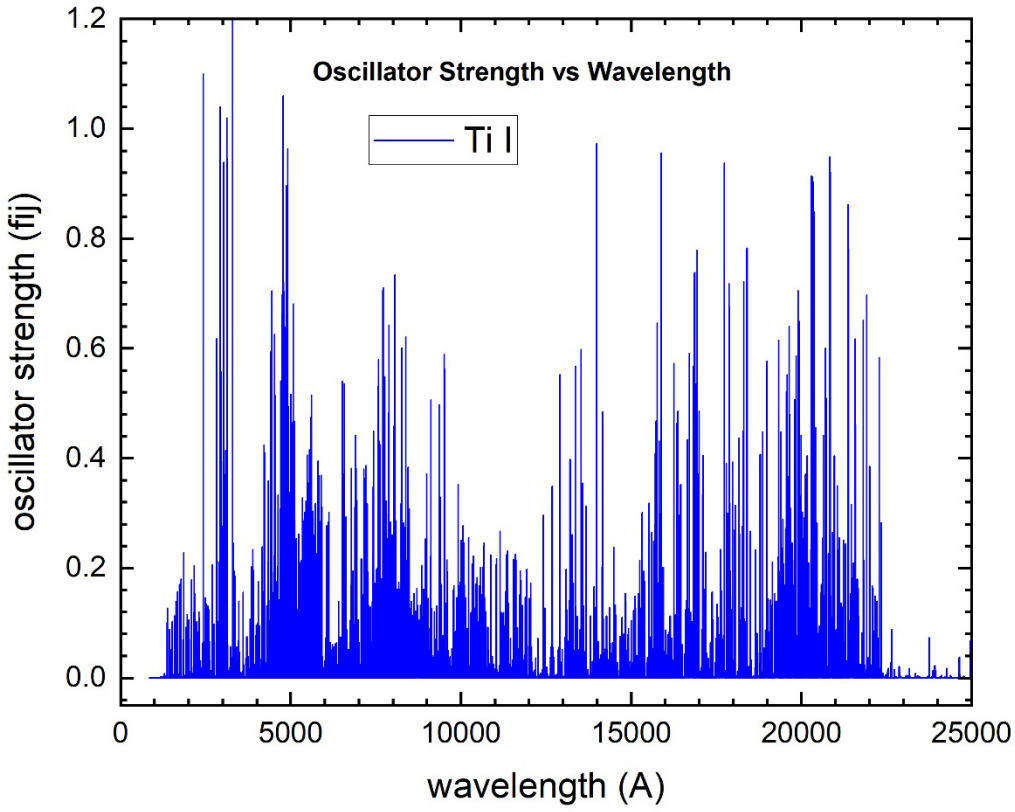

Figure 6.1: Ti I spectrum for dipole allowed oscillator strength with respect to the wavelength. A total of 77,501 transitions, both bound-bound and bound-continuum, are included. The spectrum demonstrates the strength of finding lines of Ti I in various wavelength regions

6. 6 Oscillator strength for E1 transition in Ti II

In our extensive study of Ti II, we have successfully identified a total of 969 bound fine structure energy levels. This extensive collection of energy levels served as the foundation for the computation of a significant number of transitions, encompassing both same spin and intercombination dipole allowed E1 transitions . In total, we have calculated a remarkable 101,167 transitions within the Ti II spectrum. Our electronically available dataset includes a diverse array of computed transition parameters, notably transition probabilities (A), oscillator strengths (f), and line strengths (S). These parameters are thoughtfully coupled with the corresponding level energies, collectively forming a comprehensive resource for in-depth investigations into the atomic properties and spectral behavior of Ti II.

To facilitate access to this valuable dataset, we provide a sample dataset that includes both allowed E1 and forbidden transitions (E2,M1,E3,M2) However, the complete dataset is available in an electronic format through the 'NORAD ATOMIC DATA' repository, which can be readily provided upon request.

Table 6.9: Sample table for allowed E1 same spin transitions for Ti II

```
--------------------------------------------------------------------------------
--------------------------------------------------------------------------------

  Dipole allowed E1d fine structure transitions in Breit-Pauli approx:

  Ni  Nj SLpCi SLpCj gi gj     wl(A)  Ei(Ry)   Ej(Ry)   fij       S      aji(s-1)

   1  33 4Fe 1 4Go 4  4  6   3231.77    0.00    0.28 5.84E-01  2.484E+01 2.48E+08
   2  33 4Fe 1 4Go 4  6  6   3243.81    0.00    0.28 5.29E-02  3.387E+00 3.35E+07
   3  33 4Fe 1 4Go 4  8  6   3260.88    0.00    0.28 1.13E-03  9.665E-02 9.41E+05
   5  33 4Fe 2 4Go 4  4  6   3327.98    0.01    0.28 1.68E-02  7.350E-01 6.73E+06
   6  33 4Fe 2 4Go 4  6  6   3341.65    0.01    0.28 2.71E-03  1.789E-01 1.62E+06
   7  33 4Fe 2 4Go 4  8  6   3360.63    0.01    0.28 1.19E-04  1.056E-02 9.39E+04
   2  34 4Fe 1 4Go 4  6  8   3229.87    0.00    0.28 5.27E-01  3.365E+01 2.53E+08
   3  34 4Fe 1 4Go 4  8  8   3246.79    0.00    0.28 4.82E-02  4.122E+00 3.05E+07
   4  34 4Fe 1 4Go 4 10  8   3268.84    0.00    0.28 5.81E-04  6.249E-02 4.53E+05
   6  34 4Fe 2 4Go 4  6  8   3326.86    0.01    0.28 1.46E-02  9.602E-01 6.60E+06
   7  34 4Fe 2 4Go 4  8  8   3345.67    0.01    0.28 3.13E-03  2.758E-01 1.86E+06
   8  34 4Fe 2 4Go 4 10  8   3369.59    0.01    0.28 9.92E-05  1.101E-02 7.28E+04
   3  35 4Fe 1 4Go 4  8 10   3228.98    0.00    0.28 5.23E-01  4.448E+01 2.68E+08

--------------------------------------------------------------------------------
--------------------------------------------------------------------------------
```

Table 6.10: Sample table for allowed E1 different spin transitions for Ti II

Fine structure E1i intercombination transitions in Breit-Pauli approx:

Ni	Nj	SLpCi	SLpCj	gi	gj	wl(A)	Ei(Ry)	Ej(Ry)	fij	S	aji(s-1)
9	33	2Fe 1 4Go	4	6	6	3987.80	0.05	0.28	8.57E-04	6.750E-02	3.59E+05
10	33	2Fe 1 4Go	4	8	6	4039.33	0.06	0.28	1.79E-05	1.904E-03	9.76E+03
11	33	2De 1 4Go	4	4	6	4953.43	0.10	0.28	9.40E-05	6.130E-03	1.70E+04
12	33	2De 1 4Go	4	6	6	4972.05	0.10	0.28	4.19E-06	4.113E-04	1.13E+03
14	33	4Pe 2 4Go	4	4	6	5158.33	0.11	0.28	9.64E-07	6.548E-05	1.61E+02
16	33	4Pe 2 4Go	4	6	6	5236.69	0.11	0.28	2.25E-09	2.323E-07	5.46E-01
17	33	2Ge 2 4Go	4	8	6	5253.38	0.11	0.28	5.20E-05	7.200E-03	1.68E+04
18	33	2Pe 1 4Go	4	4	6	5287.26	0.11	0.28	1.16E-07	8.085E-06	1.85E+01
21	33	4Pe 1 4Go	4	4	6	5336.40	0.11	0.28	2.46E-07	1.730E-05	3.84E+01
22	33	4Pe 1 4Go	4	6	6	5373.96	0.11	0.28	6.67E-08	7.078E-06	1.54E+01
23	33	2De 2 4Go	4	4	6	6849.44	0.15	0.28	8.86E-06	7.996E-04	8.40E+02
24	33	2De 2 4Go	4	6	6	6947.35	0.15	0.28	1.11E-06	1.527E-04	1.54E+02
27	33	2Ge 1 4Go	4	8	6	7809.64	0.17	0.28	6.71E-10	1.380E-07	9.78E-02
30	33	2Pe 2 4Go	4	4	6	10126.55	0.19	0.28	3.34E-08	4.453E-06	1.45E+00
31	33	2Fe 2 4Go	4	8	6	25210.98	0.25	0.28	5.61E-08	3.724E-05	7.85E-01
32	33	2Fe 2 4Go	4	6	6	25682.90	0.25	0.28	7.72E-07	3.915E-04	7.80E+00
9	34	2Fe 1 4Go	4	6	8	3966.75	0.05	0.28	6.89E-06	5.398E-04	2.19E+03
10	34	2Fe 1 4Go	4	8	8	4017.73	0.06	0.28	2.58E-04	2.725E-02	1.06E+05
12	34	2De 1 4Go	4	6	8	4939.37	0.10	0.28	2.67E-05	2.605E-03	5.48E+03
16	34	4Pe 2 4Go	4	6	8	5200.45	0.11	0.28	6.01E-08	6.176E-06	1.11E+01

Table 6.11: Sample table for forbidden E3 and M2 transitions for Ti II

Forbidden octu E3 and quadrupole M2 transitions in Breit-Pauli approximation:

Ni	Nj	SLpCi	SLpCj	gi	gj	wl(A)	Ei(Ry)	Ej(Ry)	SE3	AE3(s-1)	SM2	AM2(s-1)
4	33	4Fe 1 4Go	4	10	6	3283.12	4.410E-03	2.820E-01	4.99E+01	1.27E-06	0.00E+00	0.00E+00
8	33	4Fe 2 4Go	4	10	6	3384.77	1.275E-02	2.820E-01	3.61E+00	7.43E-08	0.00E+00	0.00E+00
13	33	4Pe 2 4Go	4	2	6	5149.50	1.050E-01	2.820E-01	2.05E+02	2.24E-07	0.00E+00	0.00E+00
15	33	2Pe 1 4Go	4	2	6	5229.42	1.077E-01	2.820E-01	1.33E+02	1.31E-07	0.00E+00	0.00E+00
19	33	2Ge 2 4Go	4	10	6	5302.26	1.101E-01	2.820E-01	4.69E-01	4.17E-10	0.00E+00	0.00E+00
20	33	4Pe 1 4Go	4	2	6	5314.91	1.105E-01	2.820E-01	3.38E-03	2.96E-12	0.00E+00	0.00E+00
25	33	2He 2 4Go	4	10	6	7221.74	1.558E-01	2.820E-01	2.90E+00	2.96E-10	0.00E+00	0.00E+00
26	33	2He 2 4Go	4	12	6	7304.37	1.572E-01	2.820E-01	1.48E-01	1.40E-11	0.00E+00	0.00E+00
28	33	2Ge 1 4Go	4	10	6	7821.35	1.655E-01	2.820E-01	3.62E-03	2.12E-13	0.00E+00	0.00E+00
29	33	2Pe 2 4Go	4	2	6	9975.97	1.906E-01	2.820E-01	2.11E-02	2.25E-13	0.00E+00	0.00E+00
1	34	4Fe 1 4Go	4	4	8	3217.94	0.000E+00	2.832E-01	3.62E+03	7.97E-05	0.00E+00	0.00E+00
5	34	4Fe 2 4Go	4	4	8	3313.30	8.151E-03	2.832E-01	9.05E+01	1.62E-06	0.00E+00	0.00E+00
11	34	2De 1 4Go	4	4	8	4921.00	9.800E-02	2.832E-01	2.72E+00	3.06E-09	0.00E+00	0.00E+00
13	34	4Pe 2 4Go	4	2	8	5114.46	1.050E-01	2.832E-01	1.10E+02	9.47E-08	0.00E+00	0.00E+00
14	34	4Pe 2 4Go	4	4	8	5123.16	1.053E-01	2.832E-01	2.66E+02	2.25E-07	0.00E+00	0.00E+00
15	34	2Pe 1 4Go	4	2	8	5193.28	1.077E-01	2.832E-01	8.05E+01	6.21E-08	0.00E+00	0.00E+00
18	34	2Pe 1 4Go	4	4	8	5250.32	1.096E-01	2.832E-01	1.27E+02	9.07E-08	0.00E+00	0.00E+00
20	34	4Pe 1 4Go	4	2	8	5277.59	1.105E-01	2.832E-01	2.45E-03	1.69E-12	0.00E+00	0.00E+00
21	34	4Pe 1 4Go	4	4	8	5298.77	1.112E-01	2.832E-01	4.05E-01	2.72E-10	0.00E+00	0.00E+00
23	34	2De 2 4Go	4	4	8	6787.57	1.489E-01	2.832E-01	4.35E-05	5.15E-15	0.00E+00	0.00E+00

Table 6.12: Sample table for forbidden E2 and M1 transitions for Ti II

Forbidden quad E2 and dipoe M1 transitions in Breit-Pauli approximation:

Ni	Nj	SLpCi	SLpCj	gi	gj	wl(A)	Ei(Ry)	Ej(Ry)	SE2	AE2(s-1)	SM1	AM1(s-1)
1	2	4Fe 1	4Fe 1	4	6	870985.15	0.000E+00	1.046E-03	3.18E-01	1.78E-13	9.59E+00	6.53E-05
1	3	4Fe 1	4Fe 1	4	8	362083.12	0.000E+00	2.517E-03	3.89E-02	1.31E-12	0.00E+00	0.00E+00
2	3	4Fe 1	4Fe 1	6	8	619704.79	1.046E-03	2.517E-03	4.11E-01	9.43E-13	1.29E+01	1.82E-04
2	4	4Fe 1	4Fe 1	6	10	270926.98	1.046E-03	4.410E-03	3.00E-02	3.46E-12	0.00E+00	0.00E+00
3	4	4Fe 1	4Fe 1	8	10	481380.23	2.517E-03	4.410E-03	3.69E-01	2.40E-12	1.00E+01	2.42E-04
1	5	4Fe 1	4Fe 2	4	4	111797.70	0.000E+00	8.151E-03	2.07E+01	4.98E-07	4.43E-08	2.14E-10
2	5	4Fe 1	4Fe 2	6	4	128260.99	1.046E-03	8.151E-03	2.00E+01	2.41E-07	2.53E-06	8.09E-09
3	5	4Fe 1	4Fe 2	8	4	161735.58	2.517E-03	8.151E-03	2.45E+00	9.31E-09	0.00E+00	0.00E+00
1	6	4Fe 1	4Fe 2	4	6	98287.72	0.000E+00	9.271E-03	2.00E+01	6.11E-07	1.77E-06	8.36E-09
2	6	4Fe 1	4Fe 2	6	6	110789.99	1.046E-03	9.271E-03	1.68E+01	2.82E-07	1.06E-08	3.51E-11
3	6	4Fe 1	4Fe 2	8	6	134908.81	2.517E-03	9.271E-03	2.60E+01	1.63E-07	1.59E-06	2.91E-09
4	6	4Fe 1	4Fe 2	10	6	187439.50	4.410E-03	9.271E-03	1.91E+00	2.31E-09	0.00E+00	0.00E+00
5	6	4Fe 2	4Fe 2	4	6	813349.82	8.151E-03	9.271E-03	7.24E-01	5.70E-13	9.60E+00	8.02E-05
1	7	4Fe 1	4Fe 2	4	8	84286.55	0.000E+00	1.081E-02	2.49E+00	1.23E-07	0.00E+00	0.00E+00
2	7	4Fe 1	4Fe 2	6	8	93316.98	1.046E-03	1.081E-02	2.62E+01	7.76E-07	1.37E-06	5.66E-09
3	7	4Fe 1	4Fe 2	8	8	109860.03	2.517E-03	1.081E-02	3.43E+01	4.50E-07	5.41E-09	1.38E-11
4	7	4Fe 1	4Fe 2	10	8	142346.08	4.410E-03	1.081E-02	2.35E+01	8.44E-08	2.74E-07	3.20E-10
5	7	4Fe 2	4Fe 2	4	8	342517.31	8.151E-03	1.081E-02	9.01E-02	4.01E-12	0.00E+00	0.00E+00
6	7	4Fe 2	4Fe 2	6	8	591688.96	9.271E-03	1.081E-02	9.37E-01	2.71E-12	1.29E+01	2.09E-04
2	8	4Fe 1	4Fe 2	6	10	77892.57	1.046E-03	1.275E-02	1.95E+00	1.14E-07	0.00E+00	0.00E+00

Furthermore, as part of our research, we delved into the spectrum of titanium. Specifically, we conducted an analysis involving the plotting of oscillator strength against wavelength. This graphical representation allowed us to gain a comprehensive understanding of the titanium spectrum, shedding light on the various transitions and their intensities as a function of wavelength. This investigation provided valuable insights into the spectral characteristics and behavior of titanium in this context.

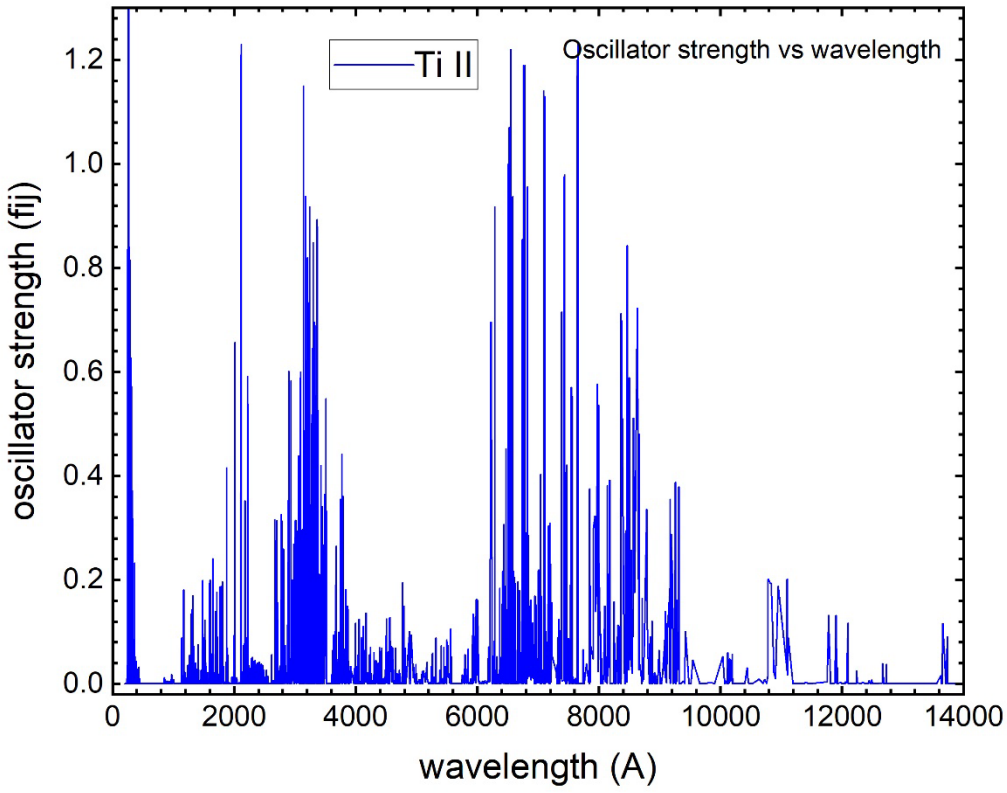

Figure 6.2: Ti II spectrum for dipole allowed oscillator strength with respect to the wavelength. A total of 101167 transitions, both bound-bound and bound-continuum, are included. The spectrum demonstrates the strength of finding lines of Ti I in various wavelength regions

6. 7 Spectral Analysis of Ti I and Ti II: Key findings

In our study, we conducted spectral analyses of Titanium I (Ti I) and Titanium II (Ti II) ions, systematically plotting oscillator strength against wavelength. The resulting figures vividly depict the strength of spectral lines for these ions at wavelengths of particular importance for applications in both astrophysical observations and the modeling of laboratory plasma environments.

These findings hold significant practical value as the identified wavelengths can be harnessed for a range of purposes. They are instrumental in the detection, analysis, and development of models in the fields of astrophysics and laboratory plasma studies. This versatility spans applications in the study of celestial bodies and their composition, as well as the design and optimization of plasma-based experiments.

Beyond their immediate utility, our research also contributes academically by deepening our understanding of the atomic properties and spectral behavior of Ti I and Ti II. This knowledge has far-reaching implications for advancing the fields of atomic physics, spectroscopy, and related scientific disciplines.

In summation, our study offers crucial insights into the spectral characteristics of Ti I and Ti II, with practical implications for astrophysical and laboratory plasma research. Simultaneously, it enriches our fundamental understanding of these elements' atomic properties and spectral behavior."

6. 8 Lifetime of Ti I

Here we investigate the lifetime of 5 fine structure level for Ti I

Table 6.13: Tabulated representation of lifetime of Ti I

Configuration	Term	*J*	lifetime (this work) (s)
$3d^2(^1D)4s4p(^3P°)$	$^3P°$	2 1 0	7.4850E-08 1.1350E-07 9.6460E-08
$3d^2(^3F)4s4p(^3P°)$	z $^3D°$	1 2	5.6050E-08 5.8530E-08

6. 9 Lifetime of Ti II

We also measured the lifetime of Ti II for 16 fine structure levels that came in good agreement with experimental work

Table 6.14: A comparison table for the lifetime of Ti II

configuration	Term	J	lifetime (This Work) (s)	lifetime (experimental) (s)
$3d^2(^3F)4p$	z $^4G°$	$^5/_2$	3.433E-09	5.7E-09 [a]
		$^7/_2$	3.418E-09	5.6E-09 [a]
		$^9/_2$	3.410E-09	5.6E-09 [a]
		$^{11}/_2$	3.407E-09	5.6E-09 [a]
$3d^2(^3F)4p$	z $^4F°$	$^3/_2$	2.676E-09	4.1E-09 [a]
		$^5/_2$	2.689E-09	4.1E-09 [a]
		$^7/_2$	2.693E-09	4.1E-09 [a]
		$^9/_2$	2.676E-09	4.1E-09 [a]
$3d^2(^3F)4p$	z $^2F°$	$^5/_2$	5.003E-09	6.8E-09 [a]
		$^7/_2$	4.979E-09	6.8E-09 [a]
$3d^2(^3F)4p$	z $^2D°$	$^3/_2$	4.541E-09	6.6E-09 [a]
		$^5/_2$	3.226E-09	6.6E-09 [a]
$3d^2(^3F)4p$	z $^4D°$	$^1/_2$	2.514E-09	3.9E-09 [a]
		$^3/_2$	2.741E-09	4E-09 [a]
		$^5/_2$	3.645E-09	4E-09 [a]
		$^7/_2$	2.516E-09	4E-09 [a]

[a] [24]

Our measurement of lifetimes for Titanium II (Ti II) ions across 16 fine structure levels demonstrated strong agreement with experimental data. This alignment validates our methodology, highlighting its accuracy and reliability. This consistency has significant implications for atomic physics, enhancing confidence in theoretical models and aiding atomic spectroscopy. Future research can build on our findings, and our work may find applications in various scientific disciplines, including astrophysics. Transparent methodology is crucial for scientific progress.

Chapter 7

Conclusion

In our research, we used a computer program called SUPERSTRUCTURE to study the energy levels of two forms of titanium: Titanium I (Ti I) and Titanium II (Ti II). We optimized the program for ten different configurations for each of these forms. While we could have used more configurations for better accuracy, doing so would have taken a lot more time and computer power. So, we chose a set of configurations that gave us good results without taking forever to compute.

Our calculations showed that the energy levels we found are pretty close to what's in the National Institute of Standards and Technology (NIST) database, especially for Ti II. However, Ti I, which has no electric charge, is more sensitive to small changes, leading to some differences. Also, the higher energy levels had more variations compared to the lower ones. This makes sense because things get more complicated at higher energies, especially when you have mixed states (a mix of different energy levels). Another reason for differences might be how SUPERSTRUCTURE and NIST assign importance to certain configurations.

We also looked at something called "transition probabilities" for both Ti I and Ti II. These probabilities tell us how likely it is for electrons to jump between energy levels. Both Ti I and Ti II had results that matched pretty well with NIST data, but Ti II was especially close. It's important to note that the NIST data we're comparing to was calculated a long time ago when computers weren't as powerful as they are today. So, the way they calculated these probabilities was different from our modern methods, which could explain some of the differences, especially for Ti I.

we looked at the spectrum of Ti I and Ti II by plotting something called "oscillator strength" against wavelength. In simple terms, this helps us understand which colors of light they emit or absorb. The spectrum of Ti II extends from the visible to the ultraviolet regions of the electromagnetic spectrum. Conversely, Ti I exhibits a broader spectrum within the wavelength range of (2000-22000) Å, characterized by a conspicuous dip in the vicinity of 12000 Å. These

findings contribute valuable insights into the spectral behavior of both titanium species, aiding in the understanding of their electronic transitions and properties in the context of the electromagnetic spectrum.

In conclusion, we conducted a meticulous assessment of the lifetime of Titanium II (Ti II). Our calculated lifetime values demonstrated a commendable alignment with experimental data, thus affirming the robustness and validity of our research endeavors.

Scope of future work

Research on the lifetimes of Titanium I (Ti I) and Titanium II (Ti II) is an essential area that merits further investigation. Currently, there is a scarcity of comprehensive information concerning the lifetimes of these atomic states.

Understanding the lifetimes of these atomic species is crucial for various scientific and technological applications. It can shed light on the stability of different energy levels, the behavior of electrons within these levels, and the interaction of these atoms with electromagnetic radiation.

Future research efforts in this direction could involve experimental measurements and theoretical calculations to determine the lifetimes of specific energy levels and transitions within Ti I and Ti II. Such investigations would not only enhance our fundamental understanding of atomic physics but also contribute to a broader range of fields, including spectroscopy, astrophysics, and materials science.

References

[1] S. G. Hacker, “The Spectrum of Arcturus,” *Astrophys J*, vol. 83, p. 140, Mar. 1936

[2] D. L. Lambert and R. E. Luck, “Isotopes of titanium in Aldebaran,” *Astrophys J*, vol. 211, p. 443, Jan. 1977,

[3] M. H. NAIMAN and R. A. PAUN, “SPECTROSCOPIC FOLLOW-UP OF THE RED SUPERGIANT STAR, BETELGEUSE,” *Rom Rep Phys*, vol. 75, p. 803, 2023.

[4] A. H. Joy, “Mira Ceti,” *Leaflet of the Astronomical Society of the Pacific*, vol. 8, no. 358, p. 57, Jan. 1959.

[5] E. Sedaghati *et al.*, “Detection of titanium oxide in the atmosphere of a hot Jupiter,” *Nature*, vol. 549, no. 7671, pp. 238–241, 2017.

[6] H. J. Hoeijmakers *et al.*, “Atomic iron and titanium in the atmosphere of the exoplanet KELT-9b,” *Nature*, vol. 560, no. 7719, pp. 453–455, Aug. 2018, doi: 10.1038/s41586-018-0401-y.

[7] A. Caulet and R. Newell, “Probing the Interstellar Medium of the Superbubble LMC2 in the Large Magellanic Cloud. I. TI II and Ca II Absorption Lines,” *Astrophysical Journal v. 465, p. 205*, vol. 465, p. 205, 1996.

[8] R. F. Bacher and S. A. Goudsmit, *Atomic Energy States as Derived from the Analyses of Optical Spectra*. McGraw-Hill, 1932.

[9] C. E. Moore, *Atomic Energy Levels as Derived from the Analyses of Optical Spectra*, no. v. 1. in Atomic Energy Levels as Derived from the Analyses of Optical Spectra. U.S. Department of Commerce, National Bureau of Standards, 1949.

[10] Y. Lyubchik, H. R. A. Jones, Y. V. Pavlenko, S. Viti, J. C. Pickering, and R. Blackwell-Whitehead, “Atomic lines in infrared spectra for ultracool dwarfs,” *Astron Astrophys*, vol. 416, no. 2, pp. 655–659, Mar. 2004

[11] W. Whaling, J. ~M. Scalo, and L. Testerman, “Transition probabilities in Ti I and the solar titanium abundance.,” vol. 212, pp. 581–590, Mar. 1977.

[12] R. ~L. Kurucz and E. Peytremann, “A table of semiempirical gf values. Pt 1: Wavelengths: 5.2682 NM to 272.3380 nm; Pt 2: Wavelengths: 272.3395 NM to 599.3892 nm; Pt 3: Wavelengths: 599.4004 NM to 9997.2746 NM,” *SAO Special Report*, Jan. 1975.

[13] G. A. Martin, J. R. , Fuhr, and W. L. Wiese, “.,” *J. Phys. Chem. Ref. Data*, vol. 15, 1988.

[14] P. L. Smith and M. Kühne, “Oscillator strengths of neutral titanium from hook method measurements in a furnace - I. Lines from the a ^{3} F $_{2, 3 \text{ and } 4}$ levels at 0, 0.021, and 0.048 eV,” *Proceedings of the Royal Society of London. A. Mathematical and Physical Sciences*, vol. 362, no. 1709, pp. 263–279, Jul. 1978,

[15] D. E. Blackwell, A. D. Petford, M. J. Shallis, and S. Leggett, “Precision measurement of relative oscillator strengths for Ti I – I. Transitions from levels a3F2 (0.00 eV) and a3F3 (0.02 eV) and a3F4 (0.05 eV) measured with an accuracy of 0.5 per cent,” *Monthly Notices of the Royal Astronomical Society*, vol. 199, pp. 21–31, 1982,

[16] N. Grevesse, A. D. Petford, and D. E. Blackwell, “Revision of the absolute scale of the Oxford TI I oscillator strengths and the solar titanium abundance,” vol. 208, pp. 157–158, 1989.

[17] D. E. Nitz, M. E. Wickliffe, and J. E. Lawler, “Atomic Transition Probabilities in Ti i,” *Astrophys J Suppl Ser*, vol. 117, no. 1, pp. 313–317, Jul. 1998

[18] S. Salih and J. E. Lawler, “lifetime of ti1 by nasa,” *Astron Astrophys*, vol. 239, pp. 407–412, 1990, Accessed: Sep. 10, 2023.

[19] J. Rudolph and V. Helbig, “Lifetimes of excited states of neutral titanium and vanadium,” 1982.

[20] H. Hartman, T. Gull, S. Johansson, and N. Smith, “Identification of emission lines in the low-ionization strontium filament near Eta Carinae,” *Astron Astrophys*, vol. 419, no. 1, pp. 215–224, May 2004

[21] H. , S. öm, C. M. , L. Z. S. , L. H. Nilsson, C. M. , L. Z. S. , Sikstr öm, and H. Lundberg, ".," *A&A*, vol. 362, p. 410, 2000.

[22] P. Palmeri *et al.*, "Lifetimes of metastable levels of singly ionized titanium: theory and experiment," *Journal of Physics B: Atomic, Molecular and Optical Physics*, vol. 41, no. 12, p. 125703, Jun. 2008,

[23] M. Kwiatkowski, K. Werner, and P. Zimmermann, "Radiative lifetimes and absolute transition probabilities in Ti ii," *Phys Rev A (Coll Park)*, vol. 31, no. 4, pp. 2695–2697, Apr. 1985

[24] A. A. Bizzarri MCE Huber Noels N Grevesse Scott D Bergeson *et al.*, "Ti-II Transition Probabilities and Radiative Lifetimes in Ti+ and the Solar Titanium abundance," *Astron. Astrophys*, vol. 273, pp. 707–718, 1993,

[25] G. , Langhans, W. , Schade, and V. Helbig, "." *Z. Phys. D At. Mol. Clusters,* vol. 34, p. 151, 1995.

[26] J. R. Roberts, T. Andersen, and G. Sorensen, "Determination of Atomic Lifetimes and Absolute Oscillator Strengths for Neutral and Ionized Titanium," *Astrophys J*, vol. 181, p. 567, Apr. 1973

[27] J. C. Pickering, A. P. Thorne, and R. Perez, "Oscillator strengths of transitions in Ti II in the visible and ultraviolet regions," *Astrophys J Suppl Ser*, vol. 132, no. 2, pp. 403–409, Feb. 2001,

[28] M. P. Wood, J. E. Lawler, C. Sneden, and J. J. Cowan, "Improved TiII log(gf) values and abundance determinations in the photospheres of the sun and metal-poor star HD 84937," *Astrophysical Journal, Supplement Series*, vol. 208, no. 2, Oct. 2013

[29] L. M. Wiese, J. A. Fedchak, and J. E. Lawler, "Absorption f-values of Ti II vacuum ultraviolet resonance transitions," *Astrophys J*, vol. 547, no. 2, pp. 1178–1183, Feb. 2001,

[30] T. M. Luke, "Transition rates in singly ionized titanium," *Can J Phys*, vol. 77, no. 8, pp. 571–583, Dec. 1999

[31] M. A. Bautista, H. Hartman, T. R. Gull, N. Smith, and K. Lodders, "[Ti ii] and [Ni ii] emission from the strontium filament of η Carinae," *Mon Not R Astron Soc*, vol. 370, no. 4, pp. 1991–2003, Jul. 2006,

[32] H. Lundberg *et al.*, "Oscillator strengths for high-excitation Ti II from laboratory measurements and calculations," *Mon Not R Astron Soc*, vol. 460, no. 1, pp. 356–362, Jul. 2016.

[33] W. Li, H. Hartman, K. Wang, and P. Jönsson, "Theoretical investigation of oscillator strengths and lifetimes in Tia II," *Astron Astrophys*, vol. 643, Nov. 2020,

[34] B. H. Bransden and C. J. Joachain, *Physics of Atoms and Molecules*. New York: (Longman Scientific and Technical, co-published with John Wiley and Sons Inc, 1990.

[35] V. Fock, "Zur Theorie des Wasserstoffatoms," *Zeitschrift für Physik*, vol. 98, no. 3–4, pp. 145–154, Mar. 1935.

[36] C. F. Fischer, *Hartree--Fock method for atoms. A numerical approach*. United States: John Wiley and Sons, Inc.,New York, 1977.

[37] W. Eissner and H. Nussbaumer, "A programme for calculating atomic structures," *Journal of Physics B: Atomic and Molecular Physics*, vol. 2, no. 10, p. 305, Oct. 1969,

[38] W. Eissner, M. Jones, and H. Nussbaumer, "Techniques for the calculation of atomic structures and radiative data including relativistic corrections," *Comput Phys Commun*, vol. 8, no. 4, pp. 270–306, 1974

[39] E. U. Condon and G. H. Shortley, *The Theory of Atomic Spectra* . London: Cambridge University Press, 1951.

[40] E. Godfredsen, "Atomic Term Energies for Atoms and Ions with 11 TO 28 Electrons," vol. 145, p. 308, Jul. 1966,.

[41] M. Jones, "Relativistic corrections to atomic energy levels," *Journal of Physics B: Atomic and Molecular Physics*, vol. 3, no. 12, pp. 1571–1592, Dec. 1970,

[42] M. Jones, “Mutual spin-orbit and spin-spin interactions in atomic structure calculations,” *Journal of Physics B: Atomic and Molecular Physics*, vol. 4, no. 11, pp. 1422–1439, Nov. 1971

[43] M. Jones, “On the use of the Breit—Pauli approximation in the study of relativistic effects in electron-atom scattering,” *Philosophical Transactions of the Royal Society of London. Series A, Mathematical and Physical Sciences*, vol. 277, no. 1273, pp. 587–622, Jan. 1975, doi: 10.1098/rsta.1975.0016.

[44] H. E. Saraph, “Fine structure cross sections from reactance matrices,” *Comput Phys Commun*, vol. 3, no. 3, pp. 256–268, Apr. 1972,

[45] J. R. Roberts, P. A. Voigt, and A. Czernichowski, “Experimentally Determined Absolute Oscillator Strengths of TI i, TI ii, and Tiiii,” *Astrophys J*, vol. 197, p. 791, May 1975